

LI, XIAOMING, M.S. Investigation of Dialysis Methods for the Complete Removal of Cl^- from Photosystem II. (2006)
Directed by Dr. Alice Haddy. 69pp.

Photosystem II (PSII), which produces oxygen using light energy, requires Cl^- as a cofactor. Cl^- appears to be difficult to remove from PSII because there always remains residual activity of 25-40%.

We have tested variations of the dialysis method to deplete PSII of Cl^- by introducing NO_3^- or Br^- before dialysis. NO_3^- pretreatment produced a preparation with suppressed activation by NO_3^- , suggesting that NO_3^- replaced Cl^- at its site of activation. Br^- pretreatment produced the preparation with the lowest residual activity and the highest total activity, indicating that it was the best method for Cl^- depletion.

The electron paramagnetic resonance (EPR) multiline signal from the S_2 state was examined in the presence of Cl^- , Br^- and NO_3^- in the Cl^- depleted PSII pretreated with NO_3^- . The signal height followed the same trend as oxygen evolution activity with $\text{Cl}^- > \text{Br}^- > \text{no anion} > \text{NO}_3^-$.

INVESTIGATION OF DIALYSIS METHODS FOR THE COMPLETE REMOVAL
OF Cl^- FROM PHOTOSYSTEM II

By

Xiaoming Li

A Thesis Submitted to
the Faculty of the Graduate School at
The University of North Carolina at Greensboro
In Partial Fulfillment
Of the Requirements for the Degree
Master of Science

Greensboro
2006

Approved by

Committee Chair

APPROVAL PAGE

This thesis has been approved by the following committee of the Faculty
of the Graduate School at the University of North Carolina at Greensboro.

Committee Chair _____

Committee Members _____

Date of Acceptance by Committee

Date of Final Oral Examination

ACKNOWLEDGEMENTS

This research was supported by the National Science Foundation, the Dreyfus Foundation and the UNCG Office of Research. I want to appreciate Dr. Alice Haddy for her support, teaching, discussions, and encouragement throughout this project.

TABLE OF CONTENTS

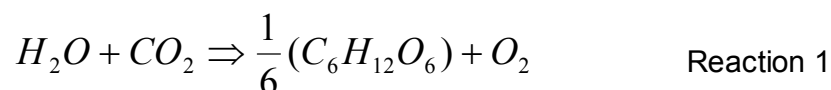
	Page
CHAPTER	
I. INTRODUCTION	1
Photosynthesis and Photosystem II	1
Structure of PS II	8
Cl ⁻ Effects in PS II	13
Electron Paramagnetic Resonance Studies	15
II. OVERVIEW OF THE STUDY	18
Measurement of the oxygen evolution activity of PS II after washings	18
Characterization of the oxygen evolution activity in PS II after Cl ⁻ depletion by dialysis and anion exchange	19
Measurement of the S ₂ state EPR signals of PS II that were Cl ⁻ depleted after NO ₃ ⁻ pretreatment	19
III. MATERIALS AND METHODS	21
General Methods	21
Treatment of PS II to remove Cl ⁻	24
Kinetic analysis of O ₂ evolution assays	25
EPR Analysis	27
IV. RESULTS	29
Overview of Objects	29
Effect of Removing Cl ⁻ from the Buffer by Washing	29
Effect of Cl ⁻ depletion of PS II by dialysis	34
SDS-PAGE analysis of PS II after dialysis	53
Study of the S ₂ state EPR signals in PS II depleted of Cl ⁻ after NO ₃ ⁻ treatment	54
V. DISCUSSION	60
REFERENCES	65

CHAPTER I

INTRODUCTION

The goal of this project is to better understand the Cl⁻ effect in the process of the photosynthetic oxygen evolution in Photosystem II (PS II).

Photosynthesis is the primary and the most important biological energy transfer process of the ecosystems on earth. It is carried out by a wide variety of organisms, such as green plants, algae, cyanobacteria and several types of more primitive non-oxygen-evolving bacteria. Photosynthesis is a process by which sunlight energy is converted into the biochemical energy needed to power life. It directly or indirectly provides all our food and most of our energy resources. The simple net reaction which shows the O₂ producing process is:



where C₆H₁₂O₆ is a glucose molecule. The reaction free energy is ΔG=+479.1 kJ·mol⁻¹, which is provided by light absorption. ⁽¹⁾

Photosynthesis and Photosystem II

The chloroplast is the organelle of photosynthesis in higher plants. ⁽¹⁾ Chloroplasts provide the energy and the reduced carbon for plant growth. A large number of reactions contribute to the overall reaction of photosynthesis

given above, and these are separated into the light reactions and dark reactions. The light reactions are initiated by the absorption of light by the reaction center, followed by charge separation. They lead to the production of ATP and the reduction of NADP⁺. Using the NADPH and ATP produced by the light reactions, the dark reactions carry out the process of the reduction of carbon dioxide to glucose which is the basic energy storage compound for living things.

Reaction Center

The photosynthetic reaction center is the complex of excitable molecules that absorbs solar radiation and initiates conversion of light energy into chemical energy. ⁽²⁾ It lies at the center of each photosystem, which is a membrane-bound protein complex. The reaction center is a pigment-protein complex, combining both chlorophylls and other electron transfer cofactors. Absorption of light energy creates an excited state of a special chlorophyll. The excited state energy is transferred to chemical changes in molecules in the reaction center. The charge separation process of the photosynthetic reaction center is:



By absorbing photon energy, the chlorophyll pigment (P) is promoted to an excited electronic state (P^{*}). The excited state easily and quickly loses an electron and an acceptor molecule (A) gains the electron immediately. The

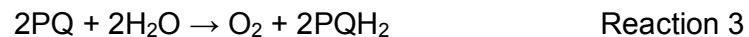
two molecules become an ion-pair state P^+A^- .

Photosystem I and II

Photosynthesis of higher plants requires two large protein complexes located in the thylakoid membranes: photosystem I (PS I) and photosystem II (PS II). Each photosystem contains a reaction center (P700 in PS I or P680 in PS II). Together PS I and PS II catalyze the light-induced steps in oxygenic photosynthesis. PS I and PS II both consist of many hydrophobic intrinsic subunits and a few extrinsic subunits. PS I contains about 100 chlorophyll a molecules, 2 phylloquinones, and 3 Fe_4S_4 -clusters. ⁽³⁾ PS I reduces the final electron acceptor, NADP⁺. PSII contains a few chlorophyll a and b molecules, 2 plastoquinones, 4 manganese ions and several other bound cofactors such as Ca^{2+} and Cl^- . PS II provides the initial electron in the electron transfer chain from the oxidation of water. PS I and PS II are linked by an electron transport chain that includes a third membrane-bound protein complex, cytochrome b_6f .

Electron transfer of PS II

Photosystem II is the only known protein complex that can oxidize water and release O_2 into the atmosphere. The general reaction equation is:



Photosystem II uses light energy to carry out the oxidation of water and the reduction of plastoquinone (PQ). There are at least five redox components involved in transferring electrons from H_2O to plastoquinone: the water

oxidizing manganese cluster (Mn)₄Ca, a tyrosine residue Tyr Z, the reaction center chlorophyll (P680), pheophytin, and the plastoquinone molecules, Q_A and Q_B. The general Photosystem II electron transport pathway is given in:

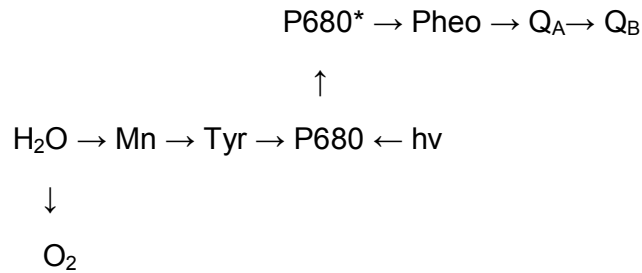


Figure 1: The electron transfer pathway in PS II

Absorbing light energy, the reaction center chlorophyll P680 is excited to P680* and transfers an electron to pheophytin, creating P680⁺/Pheo⁻. This process takes about a few picoseconds ⁽⁴⁾. After that, the electron is transferred from pheophytin to a bound plastoquinone molecule (Q_A) within 200 picoseconds. Although plastoquinone normally acts as a two-electron acceptor, Q_A is only a one-electron acceptor at first. Then the electron is transferred from Q_A⁻ to another plastoquinone molecule Q_B which is mobile. At the manganese cluster, water is oxidized and oxygen is released. Meanwhile, the electrons from water are passed to the tyrosine Tyr Z, which reduces P680⁺ to its original state. The process is repeated constantly during light excitation. Figure 2 shows how the electron transfer process takes place across the membrane.

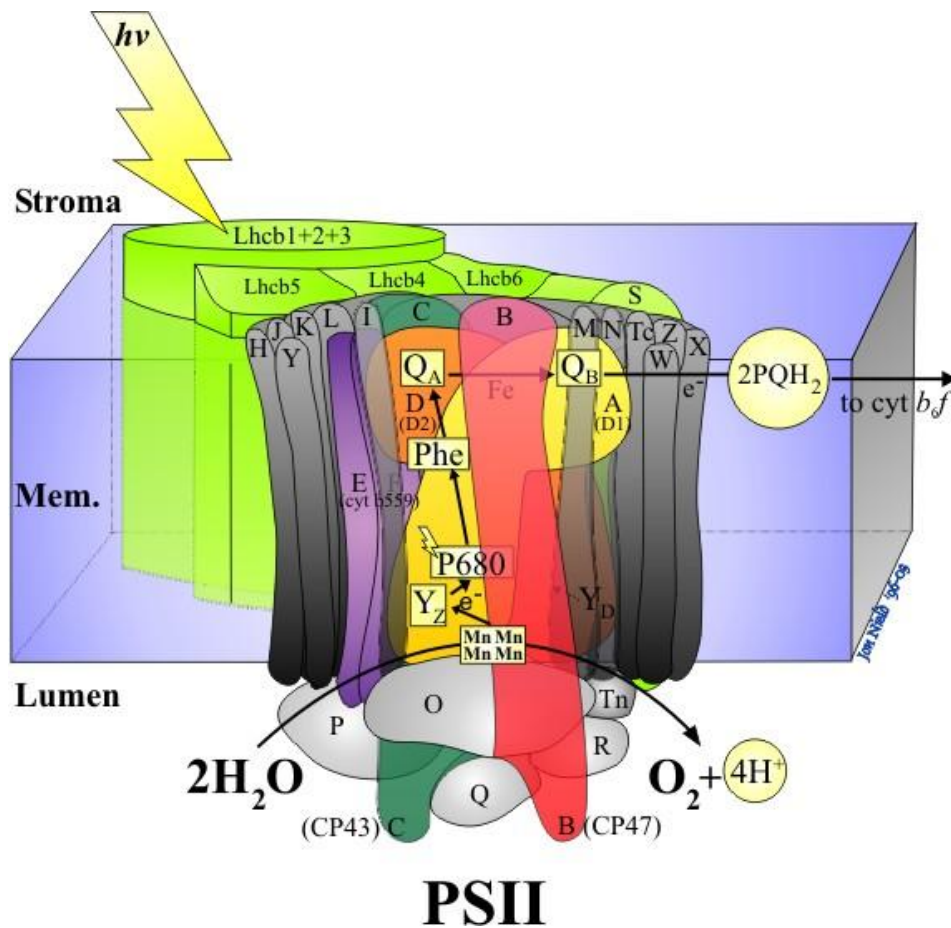


Figure 2: Schematic diagram of the electron transport chain in PS II ⁽⁵⁾

<http://www.bio.ic.ac.uk/research/barber/psliimages/PSII.html>

S-state cycle

Oxygen is produced at the oxygen evolving complex (OEC) of PS II, which includes the Mn cluster, Tyr Z, and other possible cofactors. The S-states are the oxidation states of the OEC. During water oxidation, the OEC cycles through a series of five states, known as S_i-state (i=0-4). ⁽⁴⁾ The index number (i=0-4) represents the number of stored oxidizing equivalents.

In the Kok S-state model, every PS II reaction center is considered to be an independent unit (see Figure 3).⁽⁶⁾ Light energy induces a transition between the S_n and S_{n+1} states. S_0 is the most reduced state.⁽⁴⁾ The S_1 state is the dark-stable state and the S_2 and S_3 states are intermediate states. The S_4 state, which is the highest oxidation state, is unstable and easily releases an oxygen molecule.

In the excitation process, the reaction center chlorophyll P680 absorbs a photon and is oxidized to the $P680^+$ cation, which in turn oxidizes tyrosine Y_z to Y_z^{\cdot} . After that, Y_z^{\cdot} abstracts an electron from the OEC, which induces the $S_0 \rightarrow S_1$ transition. The $S_1 \rightarrow S_2$, $S_2 \rightarrow S_3$ and $S_3 \rightarrow S_4$ transitions are also induced by the same process. Light absorption pushes the system from one S state to the next, until the S_4 state is reached. The S_4 state produces O_2 without further light input and the system returns to S_0 . The net result of this cycle is the release of an oxygen molecule and the transfer of four electrons to the quinone electron acceptor molecules of PSII.

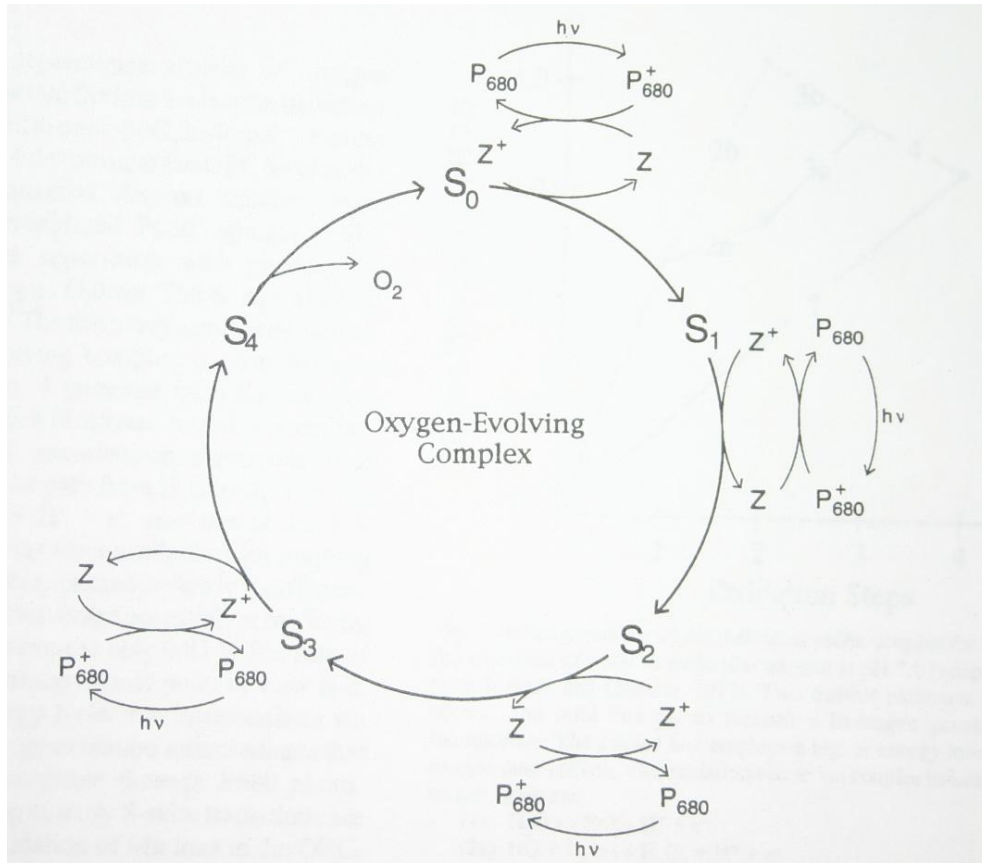


Figure 3: The OEC S-state cycle introduced by Kok et al. (1970) ⁽⁶⁾

Structure of PS II

The recent improvement of crystal quality has led to the collection of several X-ray crystallography structures of Photosystem II from the cyanobacterium, *Thermosynechococcus elongatus*.⁽⁷⁾ The crystals were fully competent in electron transport and oxygen evolution. The results show that PSII contains at least 19 subunits and there are 16 subunits located within the photosynthetic membrane. 36 chlorophyll and 7 all-trans carotenoids were found through study of the electron density map. 24 α -helices were assigned to the reaction center subunits D1 and D2, the inner-antenna subunits CP43 and CP47, and the α and β subunits of Cyt b-559. The remaining α -helices belong to smaller subunits and could not be assigned reliably. These are designated as PsbH, PsbI, PsbJ, PsbK, PsbL, PsbM, PsbN and PsbX.⁽⁸⁾ We can see the overall PS II structure in Figure 4.

D1 and D2: The D1 and D2 intrinsic subunits are located in the core of PS II. They are encoded by the *psbA* and *psbD* genes, respectively.⁽⁹⁾ The D1 and D2 subunits contain several cofactors, such as the reaction center P680, quinone acceptors Q_A , Q_B , and the redox active tyrosines TyrZ⁺ and TyrD⁺.

Cytochrome *b-559*: Cytochrome *b-559* is a heme protein, containing two subunits: the 9 kDa α subunit and the 4.5 kDa β subunit. These subunits are encoded by the *psbE* and *psbF* genes. Cytochrome *b559* can have different reduction potentials. The high potential form has reduction potential of +400

mV. ⁽¹⁰⁾

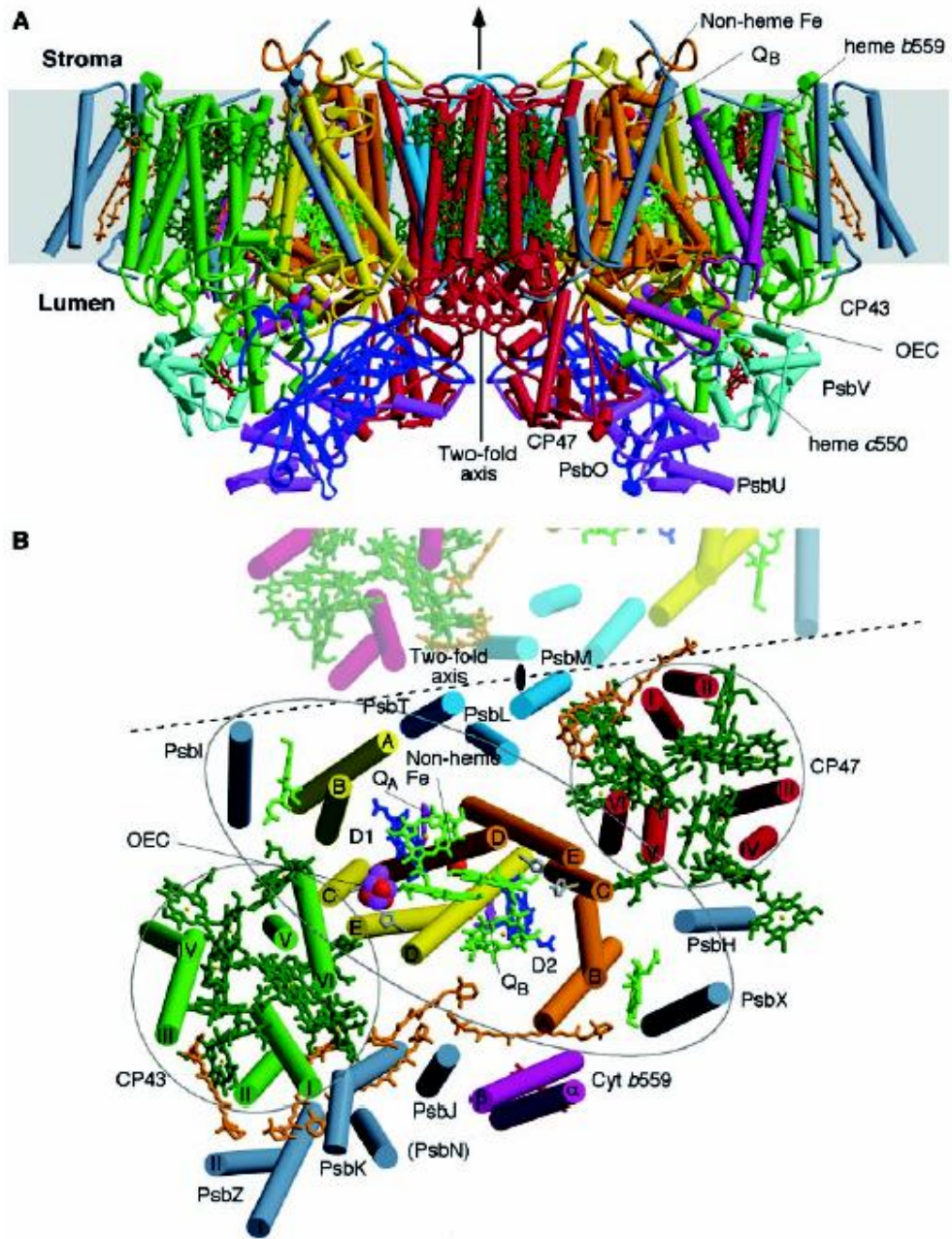


Figure 4: Crystal structure of PS II ⁽⁷⁾. (A) View of the PS II from the side (parallel to the membrane). (B) View of the PS II monomer from the top (stromal side of membrane).

CP47 and CP43: The CP47 and CP43 proteins are chlorophyll binding proteins that are closely associated with the reaction center. They contain a total of 26 antenna chlorophylls within the core complex. ⁽⁹⁾ They are encoded by the *psbB* and *psbC* genes. CP47 and CP43 serve to transfer the energy from the light-harvesting pigment proteins to the photochemical reaction center. We can see the core subunits (D1, D2, Cytochrome *b-559*, CP47 and CP43) in Figure 4.

The 17, 23 and 33 kDa Extrinsic Subunits

The three extrinsic subunits of masses 17 kDa, 23 kDa and 33 kDa, which bind on the luminal side of PS II, regulate the access of ions to the Mn cluster.

While PS II from all species contain the 33 kDa subunit, only higher plants have the 17 and 23 kDa subunits. The 33 kDa protein interacts closely with the intrinsic subunits of PS II and also plays the most important role of the extrinsic subunits. It appears to stabilize the manganese cluster even under low Cl⁻ (< 100 mM) conditions. ^(11, 12) Removal of the 33 kDa protein often results in loss of manganese.

The 23 kDa subunit associates with PSII through its interaction with the 33 kDa subunit. The 23 kDa subunit requires the 33 kDa subunit for binding to PS II and the 17 kDa subunit requires the 23 kDa subunit for binding to PS II.

^(11, 13)

The 23 and 17 kDa proteins are easily released from higher plant PSII by washing with high concentration ($> 1.0 \text{ M}$) NaCl. Removal of the 23 kDa protein results in a requirement for Ca^{2+} , which is not needed in its presence. Removal of the 23 kDa subunit also results in a more obvious requirement for Cl^- . The 23 kDa and 33 kDa proteins have a strong effect on decreasing the Cl^- concentration optimum for oxygen evolution. ^(14, 15) Removal of the 17 kDa subunit does not have a very large effect, only a slight effect on the Cl^- requirement. The 17 kDa subunit did not change the Cl^- concentration optimum clearly, although it helped to support oxygen evolution at Cl^- concentrations below 3 mM. ⁽¹⁶⁾

Oxygen Evolving Complex (OEC)

Based on the recent crystal structure by Ferreira and colleagues, the oxygen evolving complex (OEC) is thought to be a cubane-like Mn_3CaO_4 cluster, with each metal ion having three μ -oxo bridges, and with a fourth Mn ion connected by a mono- μ -oxo bridge in the extended region (Figure 5). ⁽⁶⁾ In the model of the OEC, the metal-to-metal distances within the cubane-like cluster are about 2.7 Å for Mn-Mn and 3.4 Å for Mn-Ca.

Based on the OEC structure, Ferreira and colleagues suggested that Mn-4 is a reactive Mn ion. Mn-4 was thought to be reactive because in the electron density map, it was observed to be bound by a water molecule or an oxygen intermediate. The electron density indicated that the Mn_3CaO_4 cluster

has four side chains as ligands, which have been identified as D1 Asp³⁴² for Mn-1, D1 Glu¹⁸⁹ and D1 His³³² for Mn-2, and CP43 Glu³⁵⁴ for Mn-3 (Figure 5).⁽⁶⁾

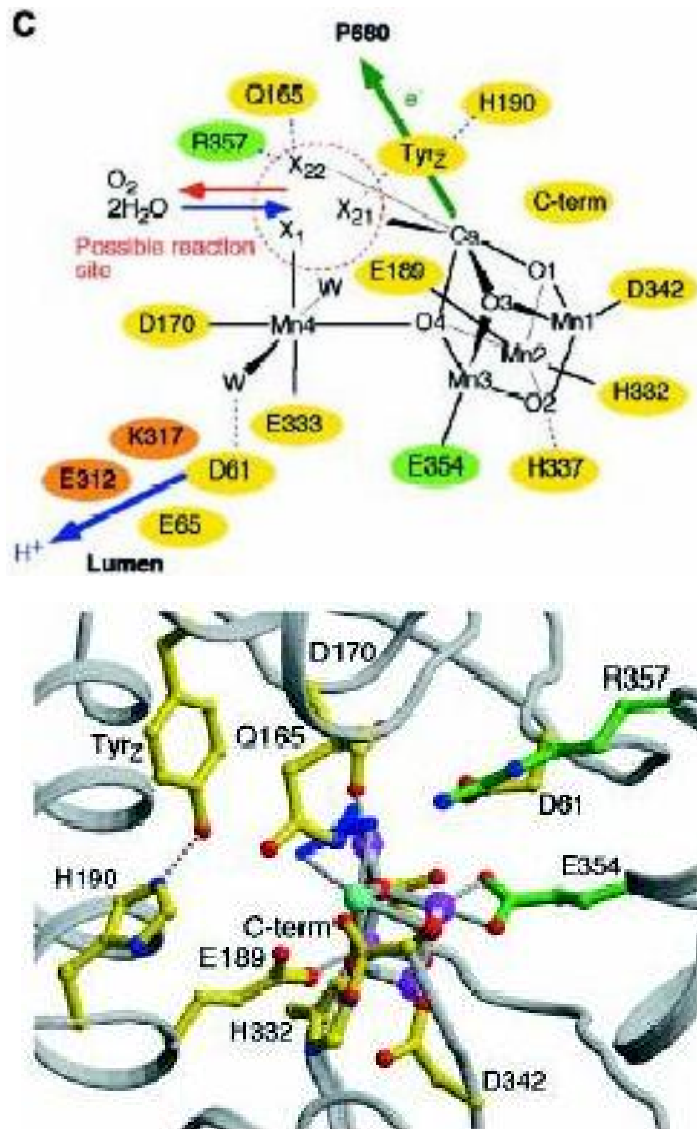


Figure 5: The oxygen-evolving center (OEC).⁽⁶⁾ Left: Schematic view of the OEC.

Right: View of the OEC with ligands. O, Mn and Ca atoms are shown in red, purple and green.

Siegbahn and colleagues found by molecular modeling that a prerequisite for the mechanism of water oxidation is a tightly bound Ca^{2+} located close to a Mn ion. ^(17, 18) They concluded that only one Mn ion binds water substrate during the S-state cycle and before dioxygen formation and that this Mn atom transforms into a highly reactive electrophilic intermediate which was hypothesized to be a Mn(IV) or a Mn (IV) oxo.

The distances found in the X-ray crystallography structure of the Mn cluster are consistent with distances previously determined using extended X-ray absorption fine structure (EXAFS). In order to determine whether some of the bridging oxygen atoms are protonated, Robblee and colleagues used EXAFS to determine that the distance between Mn-4 and the Mn-2 or Mn-3 is $\sim 3.3 \text{ \AA}$, which is a typical distance for a mono- μ -oxo bridge between Mn ions. ⁽¹⁹⁾

Cl^- Effects in PS II

As mentioned previously, Cl^- is a required cofactor for oxygen evolution by PS II. The extrinsic 17, 23 and 33 kDa proteins evidently retain Cl^- and Ca^{2+} and thereby support oxygen evolution activity.

The standard preparation method for PS II from higher plants is to use the detergent Triton X-100 to extract other membrane proteins from spinach thylakoid membranes leaving PSII-enriched membrane fragments. This preparation has more than 50% activity in the absence of Cl^- , but the activity

increases in the presence of Cl^- . The removal of the 17 and 23 kDa subunits, which is usually carried out with 1.0-2.0 M NaCl solution, results in a loss of photosynthetic oxygen evolution activity. ⁽⁸⁾ According to the experiments by Mitsue Miyao and Norio Murata, oxygen evolution activity can be restored to the original level with the addition of 10 mM Ca^{2+} , but not Mn^{2+} , Na^+ or Mg^{2+} . Ca^{2+} restoration of oxygen evolution activity has a similar effect as rebinding of the 23 kDa polypeptide, which is probably due to the retention of Ca^{2+} at the OEC by the 23 kDa protein. ⁽¹⁴⁾ The PS II samples prepared using high NaCl concentration have no activity in the absence of Cl^- .

Lindberg and coworkers used $^{36}\text{Cl}^-$ to study the exchange of Cl^- in PS II ⁽²⁰⁾. They found that the rate of binding showed a clear dependence on the Cl^- concentration, approaching a limiting value of about $3 \times 10^{-4} \text{ s}^{-1}$, similar to the release rate of chloride from membranes. This similarity in binding and dissociation rates showed that there is an intramolecular process controlling the exchange of chloride with the surrounding medium. There was also a strong relationship between the binding of Cl^- and the presence of the extrinsic polypeptides at the PS II donor side. The pH-dependence of the Cl^- requirement was associated with a pK_a of 7.5. The binding of Cl^- was prevented by competition from a few other anions, notably Br^- and NO_3^- .

From various research studies, it has been found that several anions can support O_2 evolution with different effectiveness, following this decreasing

order: $\text{Cl}^- > \text{Br}^- > \text{NO}_3^- > \text{I}^-$.⁽²¹⁾ We also regard azide N_3^- and F^- as inhibitors of oxygen evolution activity. They behave as competitive inhibitors in Cl^- activation of oxygen evolution.⁽²²⁾

Electron Paramagnetic Resonance Studies

Electron paramagnetic resonance (EPR) spectroscopy has been regarded as one of the most important methods in the study of the O_2 -evolving PSII membranes. EPR, also known as electron spin resonance (ESR), is the name given to the process of resonant absorption of microwave radiation by paramagnetic ions or molecules in the presence of a static magnetic field.⁽²³⁾

EPR spectroscopy, which was discovered by Zavoisky in 1944, has a wide range of applications in chemistry, physics, biology, and medicine. It is particularly useful for the study of organic radicals and transition metals such as Fe^{3+} , Mn^{2+} , Cu^{2+} and mixed valence metal clusters.

It was first shown in 1981 that the S_2 state produces a multiline EPR signal⁽²⁴⁾. The S_2 state signal is approximately 1900 G wide and has about 19 main lines. It was shown to arise from an antiferromagnetically coupled Mn cluster with total spin $S=1/2$, probably involving four Mn ions in the Mn(III) and Mn(IV) oxidation states.

Casey and Sauer made one of the first reports of the $g=4.1$ signal.⁽²⁵⁾ After illumination at 140 K, oxygen-evolving PS II preparations produced a 320-G-wide EPR signal centered near $g=4.1$ when observed at 10 K. As

discovered by Casey and Sauer⁽²⁶⁾, the $g=4.1$ signal is formed by lower temperature continuous illumination than is the multiline signal, with a maximal yield at 140 K. However in PS II samples warmed to 195 K, the $g=4.1$ signal appears to convert into the multiline signal.⁽⁴⁾ At 140 K, the signal was reduced or suppressed by replacement of Cl^- with F^- , but subsequent warming to 190 K did not lead to the recovery of the signal or produce the multiline signal. A breakthrough came from EPR studies of oriented PS II membranes in which the $g=4.1$ signal was stabilized by treatment with inhibitory levels of ammonia.^(26, 27) For the unique orientation in which the membrane normal was oriented parallel to the magnetic field, the $g=4.1$ signal was itself shown to have 'multiline' character, with at least 16 ^{55}Mn hyperfine lines present. This showed that the $g=4.1$ signal arises from Mn, and in particular, a multinuclear Mn cluster.

In another early study of the $g=4.1$ signal, the signal was produced by illumination of PS II membranes at 200 K.⁽²⁸⁾ Glycerol suppressed the signal intensity. The amplitude was found to oscillate with a period of four with respect to the number of flashes given at room temperature, with the maximum signal showing on the first and fifth flashes. This experiment clearly showed the association of the signal with the S_2 state.

Haddy, Kimel and Thomas studied the effects of azide on the S_2 state EPR signals.⁽²⁹⁾ Their work showed that when Cl^- was present, azide could

suppress the formation of the multiline and $g=4.1$ signals. This phenomenon meant that the normal S_2 state was not reached as before. In the absence of Cl^- , azide and fluoride had similar effects on the S_2 state EPR signals, suppression of the multiline signal and an increase and narrowing of the $g=4.1$ signal.

Lindberg and Andreasson studied the effects of Cl^- on the S_2 state signals using EPR. PS II membranes lost about 65% activity after being dialyzed against Cl^- free buffer to remove bound Cl^- . If Cl^- or Br^- was added to the Cl^- depleted PS II membranes, the original distribution of the signals was restored quickly (<30 s) but F^- did not have this effect. ⁽³⁰⁾

CHAPTER II

OVERVIEW OF THE STUDY

Based on the previous studies, we know that Cl^- is a very important cofactor in oxygen evolution by PS II. The extrinsic subunits of PS II evidently retain Cl^- at the OEC. Because of this, it is very difficult to completely remove Cl^- from intact PS II samples (i.e., PS II with the extrinsic subunits in place). Cl^- remaining in PS II complexes corresponds with residual activity that remains after Cl^- is removed from the medium.

Our original objective was to remove Cl^- in the presence of the two extrinsic subunits so that we may have an intact PS II preparation in which Cl^- dependence can be studied. One approach that we took to remove Cl^- was to introduce a second anion (Br^- , NO_3^-) that might facilitate exchange of Cl^- . These treatments resulted in preparations with sensitivity to higher concentrations of anions. Thus a second objective in the project was to characterize these preparations kinetically.

Measurement of the oxygen evolution activity of PS II after washings

To observe the effect of the removal of Cl^- from the buffer, PS II samples were washed by centrifugation in buffer without Cl^- . This provided a baseline of

Cl⁻ dependence to compare with more extensive Cl⁻ removal methods. PS II samples were washed either 2 or 8 times and the Cl⁻ dependence of each sample was characterized by kinetic analysis of the oxygen evolution activity.

Characterization of the oxygen evolution activity in PS II after Cl⁻ depletion by dialysis and anion exchange

Dialysis against Cl⁻ free buffer is a treatment that has been used in previous studies to remove Cl⁻ from intact PS II. Even after this treatment, samples show significant activity (30-40%) in the absence of Cl⁻. We tested dialysis as a method for removal of Cl⁻, with the introduction of a second anion that might facilitate Cl⁻ exchange. The anions chosen (Br⁻, NO₃⁻) are also activators of O₂ evolution. The supposition was that these anions might replace Cl⁻ at the active site, but not bind as tightly as Cl⁻.

Three dialysis treatments were carried out: one in the absence of Cl⁻ or other anion, one in which NO₃⁻ was added at the beginning of the dialysis, and one in which Br⁻ was added at the beginning of the dialysis. All three samples were characterized kinetically for activation by Cl⁻, Br⁻ and NO₃⁻. One sample was characterized by SDS-polyacryl amide gel electrophoresis (PAGE) to confirm the presence of the extrinsic subunits.

Measurement of the S₂ state EPR signals of PS II that were Cl⁻ depleted after NO₃⁻ pretreatment

Samples treated by dialysis showed inhibition of oxygen evolution

activity in the presence of high concentrations of anion. This was particularly true of the sample treated by dialysis in the presence of NO_3^- . This sample was chosen for further analysis by EPR spectroscopy. Study of the S_2 state EPR signals from the Mn cluster of the OEC was carried out to reveal more detail about the anion effects. The signals provide information about the presence of activating anion at the OEC.

CHAPTER III

MATERIALS AND METHODS

General Methods

PS II preparation

The PS II enriched thylakoid membrane fragments were prepared from fresh spinach according to standard methods. ⁽³¹⁾ Spinach was obtained as packaged, triple-washed market spinach from Harris Teeter. Selected leaves (600-800 g total) were ground with buffer containing 350 mM sucrose, 20 mM Mes-NaOH, 10 mM NaCl, pH=6.3 (buffer I) for 10-15 seconds. The ground spinach was strained through four layers of nylon cheese cloth and the liquid was centrifuged for 5 minutes in a Beckman JA10 rotor at 5 k rpm. The pellet was suspended in buffer containing 20 mM Mes-NaOH, 5 mM MgCl₂, 15 mM NaCl, pH=6.3 (buffer II) and centrifuged for 8 minutes (JA 10, 6.5 k rpm). The suspension was homogenized in Kimax homogenizer using a Wheaton overhead stirrer. The chlorophyll concentration was adjusted to 2.5 mgChl/ml and 1/4 the volume of 25% Triton X-100 in Buffer II was added in the dark. The sample was incubated on ice in the dark for 30 minutes. The preparation was then centrifuged for 30 minutes (JA 20, 20 k rpm). The sample was resuspended in 400 mM sucrose, 20 mM Mes-NaOH, 15 mM NaCl, pH=6.3

(buffer IV) and centrifuged for 10 seconds (JA 20, 10 k rpm) to remove granular starch. The supernatant was transferred to new tubes and centrifuged for 25 minutes (JA 20, 20 k rpm). The pellets were resuspended in buffer IV and washed by centrifugation three times. The final pellet was diluted to about 10 mgChl/ml and stored in liquid nitrogen.

Preparation of NaCl washed PS II samples

Intact PS II was thawed in a microfuge tube at room temperature. The sample was suspended in buffer containing 1.5 M NaCl, 0.4 M sucrose and 20 mM Mes-NaOH, pH=6.3.⁽¹⁴⁾ This was placed on ice for 60 minutes and then was washed three times in buffer containing 0.4 M sucrose, 40 mM Mes-NaOH and 10 mM CaCl₂, pH=6.3 by centrifuging in an Eppendorf microfuge for 3 minutes at 14 k rpm. The concentration was adjusted to 0.5 mg Chlorophyll per ml (mgChl/ml). The resulting PS II samples, which were depleted of the 17 and 23 kDa subunits, were stored in liquid nitrogen.

O₂ evolution assays

Oxygen evolution assays of PS II samples were carried out using a Clark-type O₂ selective electrode system (Yellow Springs Instruments 5331 oxygen probe) (see Figure 8). This system included a Fiber-Lite series 180 high intensity illuminator (Dolan-Jenner Industries, Inc.) and a projector lamp (300 W).

A fresh O₂ permeable membrane was placed on the Pt electrode before

each day's experiments. Assays were carried out at 25°C in a water-jacketed glass cell. Calibration was carried out using air-saturated deionized water (260 $\mu\text{M O}_2$) and water purged of O_2 by N_2 gas (zero O_2).



Figure 8: Oxygen evolution assay system

A: water bath, B: timer, C: computer, D1: Fiberlite illuminator, D2: Projector illuminator, E: reaction cell, F: electrode monitor

PS II pellets were thawed at room temperature and the chlorophyll concentration adjusted to ~ 1.5 mg /ml by adding buffer (0.4 M sucrose and 20 mM Mes-NaOH, pH=6.3). The samples were kept on ice until use. Assays were carried out in buffer (0.4 M sucrose and 20 mM Mes-NaOH, pH=6.3) containing the specified concentration of NaCl, NaBr or NaNO_3 .

1.00 ml assay buffer and 30 μ l PS II sample were combined in the sample chamber. After two minutes equilibration time, 20 μ l of 50 mM phenyl-p-benzoquinone (PPBQ) was added to the chamber to function as the electron acceptor. The sample was then illuminated with saturating white light. The oxygen evolution rates were determined from the slope of the Pt cathode voltage vs time, using a computer system (S. Baranov) for both data collection and rate calculation. Reported oxygen evolution rates are the averages of at least three measurements.

SDS-Polyacrylamide Gel Electrophoresis

SDS polyacrylamide gel electrophoresis (PAGE) in a mini gel apparatus (E-C Corporation) was carried out by the method of Kashino et al. ⁽³³⁾, using 13% gels. PS II samples were combined with 2X SDS sample buffer containing 0.1 M Tris, pH=7.5, 3% SDS, 20% glycerol, 0.10 mg/ml bromophenol blue, and incubated at 37°C for 20 min. About 10 μ g of chlorophyll were loaded onto each lane of the gel. PS II samples included intact PS II, NaCl-washed PS II, PS II Cl⁻ depleted by dialysis after NO₃⁻ pretreatment, and a molecular weight standard (Sigma Diagnostics).

Treatment of PS II to remove Cl⁻

Removal of Cl⁻ from the buffer by washing

PS II was washed by centrifugation to remove Cl⁻ from the buffer. Intact PS II was thawed at room temperature and suspended to 5.0 mgChl/ml in a

microfuge tube in buffer containing 0.4 M sucrose, 20 mM Mes, pH=6.3. The sample was then microfuged (14 k rpm, 2 min) to pellet and the supernatant was removed. The sample was then resuspended in the buffer and washed again, for a total of either 2, 6 or 8 washings. The sample was resuspended to 1.5 mgChl/ml for O₂ evolution assays.

Cl⁻ depletion of PS II by dialysis

PS II was depleted of Cl⁻ by dialysis as described by Lindberg and Andreasson, ⁽²⁰⁾ with the modification that the PS II was pretreated with Br⁻, NO₃⁻ or no anion (as control). The steps for NO₃⁻ pretreatment were as follows: PS II samples were placed in a centrifuge tube and suspended in 30-35 ml buffer (0.4 M sucrose, 20 mM Mes, pH=6.3) containing 15 mM NaNO₃. This was centrifuged 10 minutes (JA 20 rotor, 13 k rpm). This wash was repeated once with 15 mM NaNO₃, then twice more with 1 mM NaNO₃. The sample was transferred to 12,000 Dalton molecular weight cutoff dialysis bags and placed in 1 liter of buffer (0.4 M sucrose, 20 mM Mes, pH=6.3) to stir slowly at 4-5°C for 24 hours. The buffer was changed once during the dialysis. After dialysis, the samples were stored until O₂ evolution assays.

Kinetic analysis of O₂ evolution assays

Kinetic analysis of PS II washed to remove Cl⁻

Activation of PS II by anions (Cl⁻, Br⁻ or NO₃⁻) was analyzed using a modification of the Michaelis-Menten equation. Anion was treated as the

substrate for this analysis. For PS II that was washed to remove Cl⁻ from the buffer the following modification of the Michaelis-Menten equation was used:

$$V = V_0 + \frac{V_{\max}[\text{Cl}^-]}{K_M + [\text{Cl}^-]} \quad \text{Equation 4}$$

where V is the velocity of oxygen evolution activity; V₀ is the velocity of oxygen evolution activity when [Cl⁻] is zero; V_{max} is the limiting velocity as substrate concentrations become very large; [Cl⁻] is the concentration of Cl⁻ in the buffer; K_M, which is called the Michaelis constant, is the concentration of substrate that leads to half-maximal velocity. In this modification, V₀ was introduced to account for residual activity that could not be removed by washing in Cl⁻ free buffer.

Kinetic analysis of Cl⁻ depleted PS II

For PS II that was Cl⁻ depleted by dialysis (with and without anion pretreatment), activation curves were analyzed using the following modification of the Michaelis-Menten equation:

$$V = \frac{V_{\max} X}{K_M + X + X^2/K_i} + \frac{V_0}{1 + X/K_i} \quad \text{Equation 5}$$

where the V, V₀, V_{max} and K_M are defined as in Equation 4; X is the concentration of added anion; K_i is the dissociation constant of inhibition.

This equation accounts for inhibition by the activating anion from a second site (X²/K_i term). It also includes inhibition of the fraction of sample that

accounts for the residual activity ($V_0/(1 + [X]/K_i)$ term). For the analysis, V_0 was set to the value measured at zero anion added.

Data were fitted to the analytical equation using the program Sigma Plot, version 8.0. Reported errors for the fitted parameters were standard errors calculated by the program.

EPR Analysis

Preparation of Cl⁻ depleted PS II samples for EPR spectroscopy

For analysis by EPR spectroscopy, we selected the PS II preparation that was Cl⁻ depleted by dialysis after NO₃⁻ pretreatment. The PS II samples were thawed at room temperature and transferred into four 40 ml centrifuge tubes. The samples were diluted with buffer (0.4 M sucrose, 20 mM Mes, pH=6.3) containing 25 mM NaCl, NaBr, NaNO₃ or no added anion. The samples were placed on ice for 60 minutes. After that, they were centrifuged for 10 minutes (JA20, 13 k rpm) and resuspended in buffer twice. The PS II pellets were suspended to a final concentration of ~5 mg/ml and were transferred into 4 mm outer diameter clear fused quartz EPR tubes (Wilma Glass) using a length of intramedic tubing attached to a 1 cc syringe (Becton Dickinson and Company). Finally, the samples were incubated in the dark on ice for ~1 hour to produce mostly the S₁ state. Samples were then frozen and stored in liquid nitrogen.

Measurement of the S₂ state EPR signals

The S₂ state EPR signals were measured using a Bruker Instruments EMX EPR spectrometer, which operated at 9.5 GHz. PS II samples, which had been dark adapted to produce the S₁ state, were illuminated at 195 K for 8 min to produce the S₂ state. Temperature was controlled using a solid CO₂/ethanol bath. EPR spectra were taken both before and after illumination. Signal heights were measured in the illuminated-minus-dark adapted difference spectra.

The multiline signal's height was measured as the average of the 2nd, 3rd and fourth peaks that are down field from the center of the signal. Since the various samples had different chlorophyll concentrations, the heights were normalized according to concentration with the Cl⁻-containing sample regarded as the standard. The normalized heights were reported as the percentage with respect to the Cl⁻-containing sample as 100%.

CHAPTER IV

RESULTS

Overview of Objects

When the 17 and 23 kDa subunits are bound to PS II, they have the effect of retaining Cl^- within the PSII complex and their presence appears to prevent complete removal of Cl^- . This makes the study of Cl^- dependence more difficult when they are bound. We are interested in preparing PSII that is free of Cl^- in the presence of the two extrinsic subunits so that we may have an intact PS II preparation in which Cl^- dependence can be studied.

In this study, we compared variations of the dialysis method for removing Cl^- from PS II and analyzed the kinetics of oxygen evolution activity after each treatment. A major goal of this research was to reduce the residual activity of PS II in the absence of Cl^- since this is thought to reflect the presence of bound Cl^- . In the course of the study, the activation characteristics were found to be altered depending on the anion treatment, so this was analyzed in detail. In addition, to better understand the altered kinetic behavior, we measured the EPR signals of PS II depleted of Cl^- after NO_3^- treatment.

Effect of Removing Cl^- from the Buffer by Washing

The kinetics of Cl^- activation after washing PS II in buffer without added

anion was studied to provide a baseline measure of the effect of the removal of Cl^- from the buffer. PS II particles were washed twice in a microfuge tube using buffer without any chloride or other activating anions, as described in Material and Methods. The residual concentration of Cl^- in the buffer was estimated to be lower than 100 μM . The oxygen evolution activity of the sample was measured in buffer containing different concentrations of Cl^- between 0 and 25.0 mM (Figure 9A). After washing with buffer, PS II samples lost some activity probably because they lost some Cl^- . Oxygen evolution activity was restored by adding the activator anion, Cl^- .

We tested whether additional washings could remove more Cl^- , which would have an effect on the residual activity of PS II. We carried out the same experiment except washing the PS II particles 8 times in buffer without anion (Figure 9B).

Using Sigma Plot, the data for both experiments were fitted to the modified Michaelis-Menten Equation 4, which included a constant V_0 to represent the initial velocity of oxygen evolution activity when $[\text{Cl}^-]$ was zero (Table 1). Using 2 and 8 washings, V_0 was found to be 240 and 370 $\mu\text{moles O}_2\text{hr}^{-1}\text{mgchl}^{-1}$, respectively. Comparing as a percentage of the total activity, $V_0/(V_0+V_{\text{max}})$, the residual activity was found to be 0.59 and 0.63 for 2 and 8 washings, respectively. This showed that the washed PS II samples still retained about 60% activity. More than 2 washings did not lower the relative

activity any further. This suggests that there was no significant effect on Cl⁻ removal from increasing the number of washings.

Table 1: Cl⁻ activation kinetics of O₂ evolution in PS II after removal of Cl⁻ by washing

Times Washed	V ₀ (μmoles O ₂ hr ⁻¹ mgchl ⁻¹)	V _{max} (μmoles O ₂ hr ⁻¹ mgchl ⁻¹)	K _M (mM)	$\frac{V_0}{V_0 + V_{max}}$
2	240 ± 7.4	170 ± 8.5	0.64 ± 0.12	0.59
8	370 ± 9.1	210 ± 10	0.35 ± 0.06	0.63

* Reported errors for the fitted parameters were standard errors calculated by the program.

The values of V_{max} and K_M were fairly close for the two PS II samples. V_{max} was slightly higher after 8 washings, but this increase is similar to that of V₀ which suggests that this was due to other experimental factors such as the illumination. K_M was found to be 0.64 mM and 0.35 mM for 2 and 8 washings, respectively. These values of K_M are significantly different, based on the experimental error. Thus it appears that activation required a lower concentration of Cl⁻ after 8 washes.

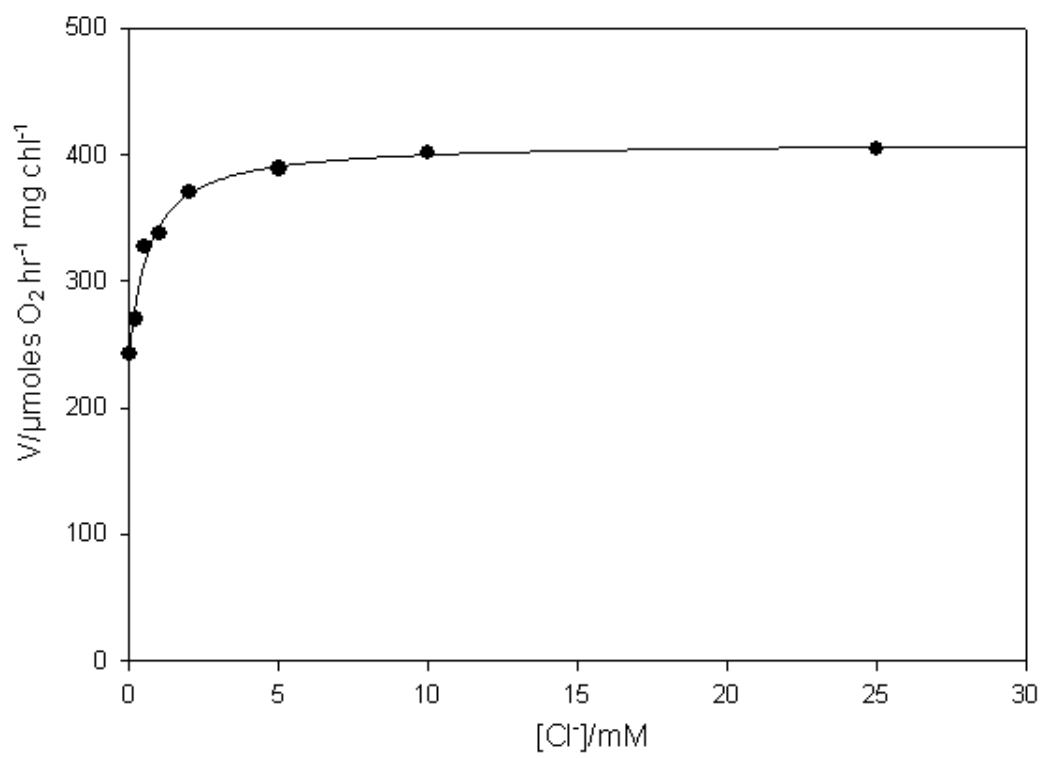


Figure 9A: Activation by Cl^- of PS II after 2 washings in Cl^- free buffer

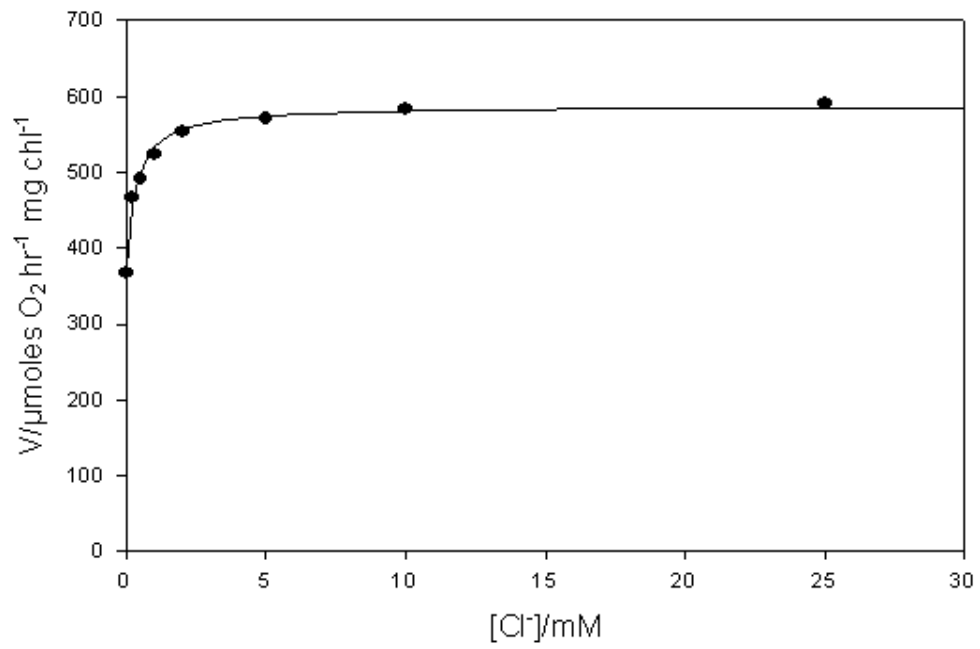


Figure 9B: Activation by Cl^- of PS II after 8 washings in Cl^- free buffer

Effect of Cl⁻ depletion of PS II by dialysis

In these experiments, we attempted to remove Cl⁻ from intact PS II through the dialysis process. We tested variations of the dialysis method for the removal of Cl⁻ from intact PS II, including no pretreatment of PS II and treatment of PS II with NO₃⁻ or Br⁻ to exchange for Cl⁻. After dialysis, the kinetics of activation of oxygen evolution activity by Cl⁻, Br⁻ and NO₃⁻ was determined for each preparation.

Intact PS II, preparations were depleted of Cl⁻ by dialysis against Cl⁻ free buffer after three different pretreatments: 15 mM NaNO₃, 15 mM NaBr or no added anion as described in Materials and Methods. A fourth PS II preparation was washed with Cl⁻ free buffer six times to remove Cl⁻ from the buffer, similar to the treatment of the last section.

For each preparation, the kinetics of activation by Cl⁻, Br⁻ and NO₃⁻ was studied. The dependence of activation on anion concentration is shown for the preparation pretreated with NO₃⁻ (Figure 10A-10C), the preparation pretreated with Br⁻ (Figure 11A-11C), the preparation without pretreatment (Figure 12A-12C), and the preparation that was washed only (Figure 13A-13C). The data were analyzed according to Equation 2, which takes into account both activation and inhibition by the anion. The results of the analysis are shown in Table 2 and Table 3 where Table 2 shows the values of the parameters with errors and Table 3 shows the same parameters but with velocities V_{\max} and V_0

presented as relative values. In each case, activation at low anion concentrations was followed by inhibition at higher anion concentrations. This behavior is typical of inhibition by the substrate from a second site. The maximum activity was generally observed between 5 and 20 mM added anion.

The experimental error was generally high because three parameters (K_M , K_I and V_{max}) were needed to fit the data to Equation 5. There was much overlap between the regions where activation and inhibition occurred, so the two effects were not well resolved. This was also the reason why V_{max} was greater than the observed maximum V .

In general, the values of V_{max} for activation by all anions for PS II, Cl^- depleted by NO_3^- exchange were lower than for any other preparation. The V_{max} values for PS II, Cl^- depleted by Br^- exchange were higher than any other preparation.

In each preparation, V_{max} was found to be the highest for activation by Cl^- , followed by Br^- , then NO_3^- . The only exception to this was the Cl^- depleted preparation with Br^- pretreatment, which showed a slightly higher V_{max} for Br^- , than for Cl^- . All three anions were good activators, with NO_3^- showing at least 70% the V_{max} of Cl^- .

Values of K_M for all preparations were similar for all three activating anions, showing values around 1 mM. The major exception was the K_M for NO_3^- activation in the NO_3^- pretreated preparation. This showed $K_M = 8.4$ mM,

which was significantly higher than the others. This indicated that NO_3^- was an exceptionally poor activator for that preparation. This was due to an increase in K_M to 8.4 mM. This observation could be explained as follows: NO_3^- may have displaced tightly bound Cl^- during dialysis, producing the residual activity after Cl^- depletion. Addition of NO_3^- did not activate further, but only inhibited. Activation by Br^- or Cl^- was observed since these anions were able to displace bound NO_3^- .

Values of K_I showed a similar trend in all preparations tested. Cl^- and Br^- showed relatively high values, between 150 and 350 mM, with the value for Cl^- higher in each case. NO_3^- on the other hand, showed a relatively low value around 60-70 mM for each preparation. This indicated that NO_3^- was more inhibitory than Cl^- or Br^- for each preparation by at least a factor of three. PS II depleted of Cl^- by exchange with NO_3^- was particularly susceptible to inhibition by NO_3^- (Figure 10C). This is because little activation was observed for this preparation.

Comparison of the K_M and K_I values for activation by Cl^- and Br^- between the various preparations revealed that NO_3^- pretreatment resulted in the lowest K_M values and highest K_I values. This indicates that when we used NO_3^- to exchange for Cl^- , the inhibition by Cl^- and Br^- was lowest and their activation was most efficient.

In the experiments using PS II pretreated with Br^- , Br^- showed a slightly

higher V_{\max} value than Cl^- but Br^- and Cl^- showed the same K_M values. These values suggest that Br^- played the same role as Cl^- in its ability to restore the PS II activity. However, Br^- had a slightly lower K_i value than Cl^- , which meant Br^- was slightly more inhibitory.

In the experiments using PS II pretreated with Br^- , the total activity (V_0+V_{\max}) was much higher than in any other preparation, exceeding 1000 $\mu\text{molO}_2/\text{mgChl}\cdot\text{hr}$. This may indicate that exchange with Br^- protected the PS II from loss of activity during the dialysis. However the high rates are still higher than expected for a control preparation, which is 500-800 $\mu\text{molO}_2/\text{mgChl}\cdot\text{hr}$. This was probably due to a systematic error, such as in the chlorophyll concentration. The relatively high rates were also promoted by the use of a new light bulb in the illuminator. While systematic error of this type may result in values of V_0 and V_{\max} that are too high, their relative values would not be affected. The values of K_M and K_i are also not affected by systematic error. Therefore it is significant that the ratio of V_0/V_0+V_{\max} is much lower for the PS II preparation that was Cl^- depleted by Br^- pretreatment than for any other preparation. This indicates that Br^- pretreatment was more successful in removing residual activity than any other treatment. Similarly, the NO_3^- pretreatment was the least successful in removing residual activity.

In general, for all PS II samples, the smallest V_{\max} value, the largest K_M value and the lowest K_i value was found for activation by NO_3^- . This showed

that it was the worst anion in the ability to restore the PS II activity compared with Cl^- and Br^- .

Table 2: Kinetic constants with standard error for activation by Cl⁻, Br⁻ or NO₃⁻ in**various Cl⁻ depleted PS II preparations**

Activating anion	V ₀	V _{max}	K _M (mM)	K _I (mM)
Cl ⁻ depleted by NO ₃ ⁻ exchange				
Cl ⁻	149	65 ± 6.6	0.17 ± 0.37	350 ± 79
Br ⁻		55 ± 7.7	0.23 ± 0.51	300 ± 74
NO ₃ ⁻		54 ± 40	8.4 ± 9.8	62 ± 22
Cl ⁻ depleted by Br ⁻ exchange				
Cl ⁻	464	720 ± 63	0.48 ± 0.36	220 ± 62
Br ⁻		790 ± 80	0.48 ± 0.41	170 ± 47
NO ₃ ⁻		580 ± 59	1.0 ± 0.46	75 ± 12
Cl ⁻ depleted by no anion buffer				
Cl ⁻	154	110 ± 17	0.82 ± 0.71	160 ± 39
Br ⁻		84 ± 15	1.4 ± 1.0	150 ± 34
NO ₃ ⁻		79 ± 33	2.4 ± 2.7	59 ± 18
Cl ⁻ removed by 6 times washings				
Cl ⁻	453	420 ± 17	0.79 ± 0.20	330 ± 45
Br ⁻		360 ± 23	0.73 ± 0.31	260 ± 43
NO ₃ ⁻		320 ± 25	0.72 ± 0.30	61 ± 5.2

* Reported errors for the fitted parameters were standard errors calculated by the program.

Table 3: Kinetic constants for activation by Cl⁻, Br⁻ or NO₃⁻ in various Cl⁻ depleted

PS II preparations

Activating anion	V _{max}	$\frac{V_0}{V_0 + V_{max}}$	K _M (mM)	K _I (mM)
Cl ⁻ depleted by NO ₃ ⁻ exchange				
Cl ⁻	100%	0.70	0.17	350
Br ⁻	86%	0.73	0.23	300
NO ₃ ⁻	84%	0.73	8.4	62
Cl ⁻ depleted by Br ⁻ exchange				
Cl ⁻	100%	0.39	0.48	220
Br ⁻	109%	0.40	0.48	170
NO ₃ ⁻	81%	0.44	1.0	75
Cl ⁻ depleted by no anion buffer				
Cl ⁻	100%	0.59	0.82	160
Br ⁻	77%	0.65	1.4	150
NO ₃ ⁻	72%	0.66	2.4	59
Cl ⁻ removed by 6 times washings				
Cl ⁻	100%	0.52	0.79	330
Br ⁻	86%	0.56	0.73	260
NO ₃ ⁻	76%	0.59	0.72	61

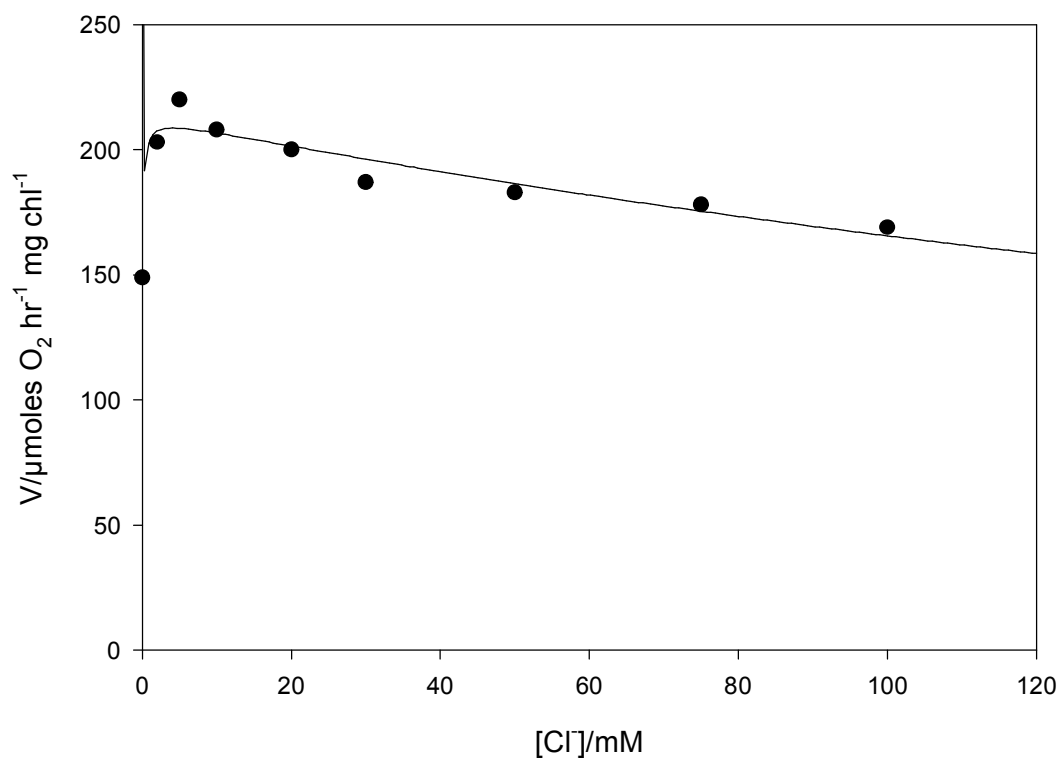


Figure 10A: Cl⁻ activation of PS II that was Cl⁻ depleted by dialysis after NO₃⁻ treatment

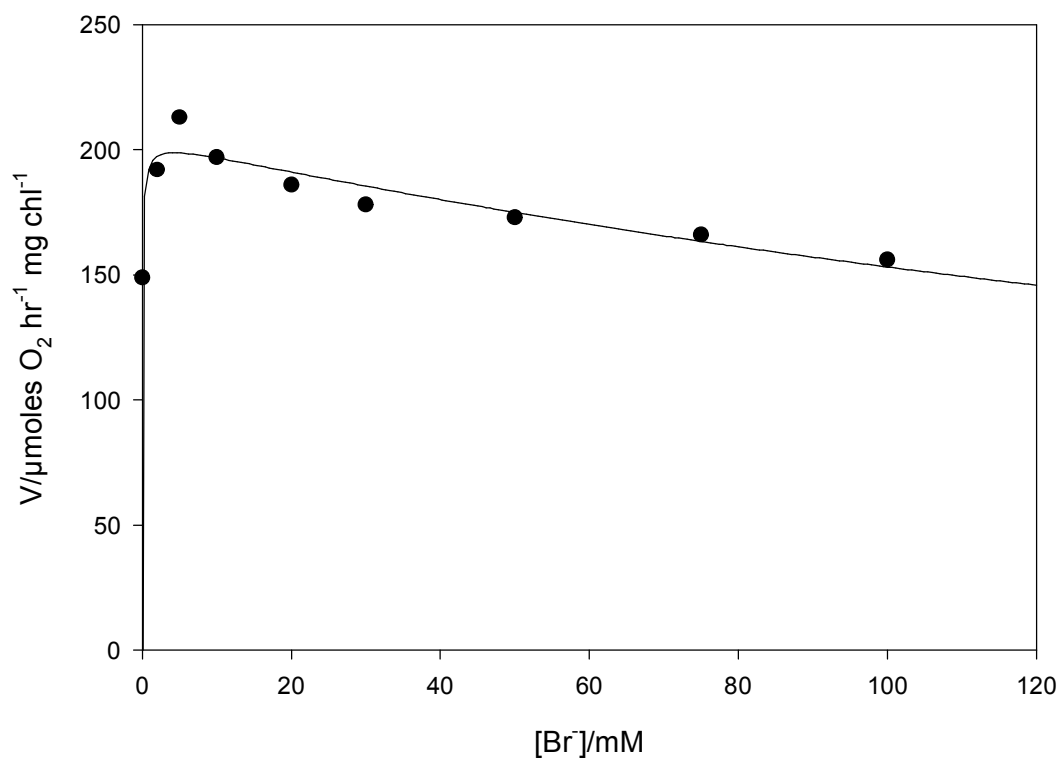


Figure 10B: Br⁻ activation of PS II that was Cl⁻ depleted by dialysis after NO₃⁻

treatment

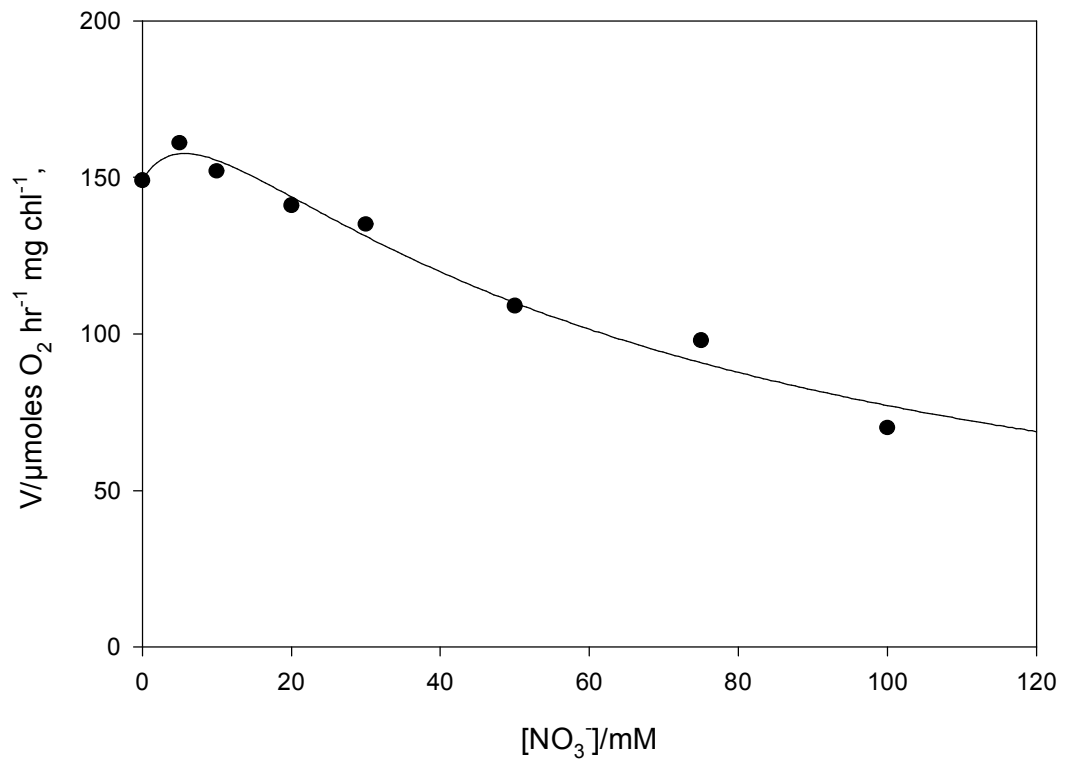


Figure 10C: NO₃⁻ activation of PS II that was Cl⁻ depleted by dialysis after NO₃⁻ treatment

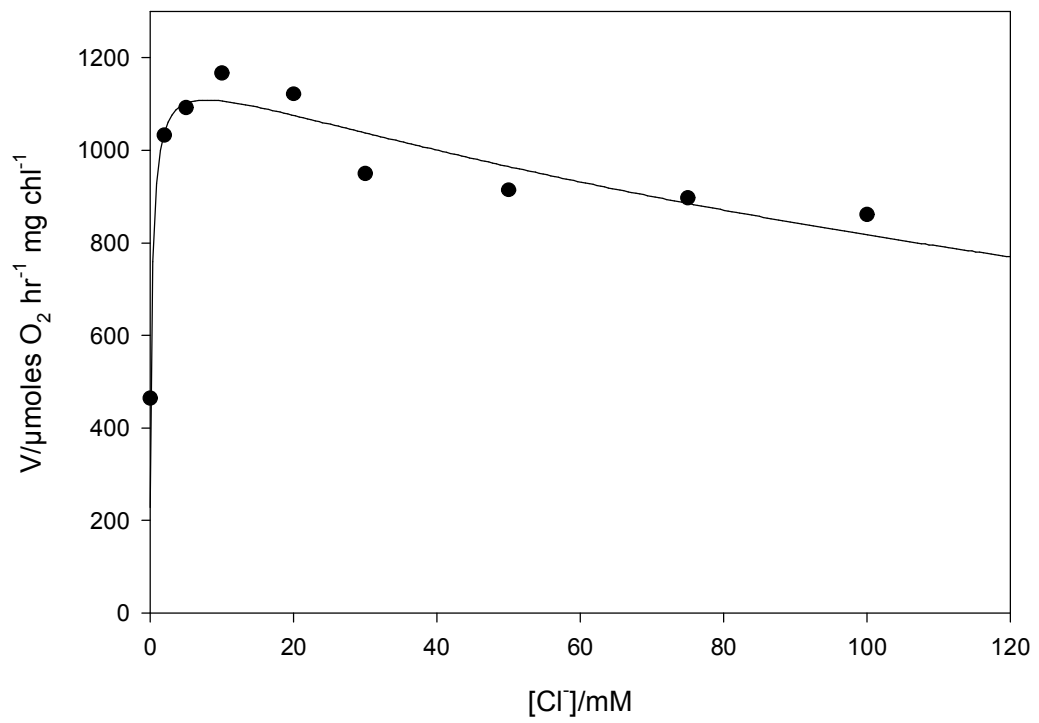


Figure 11A: Cl⁻ activation of PS II that was Cl⁻ depleted by dialysis after Br⁻ treatment

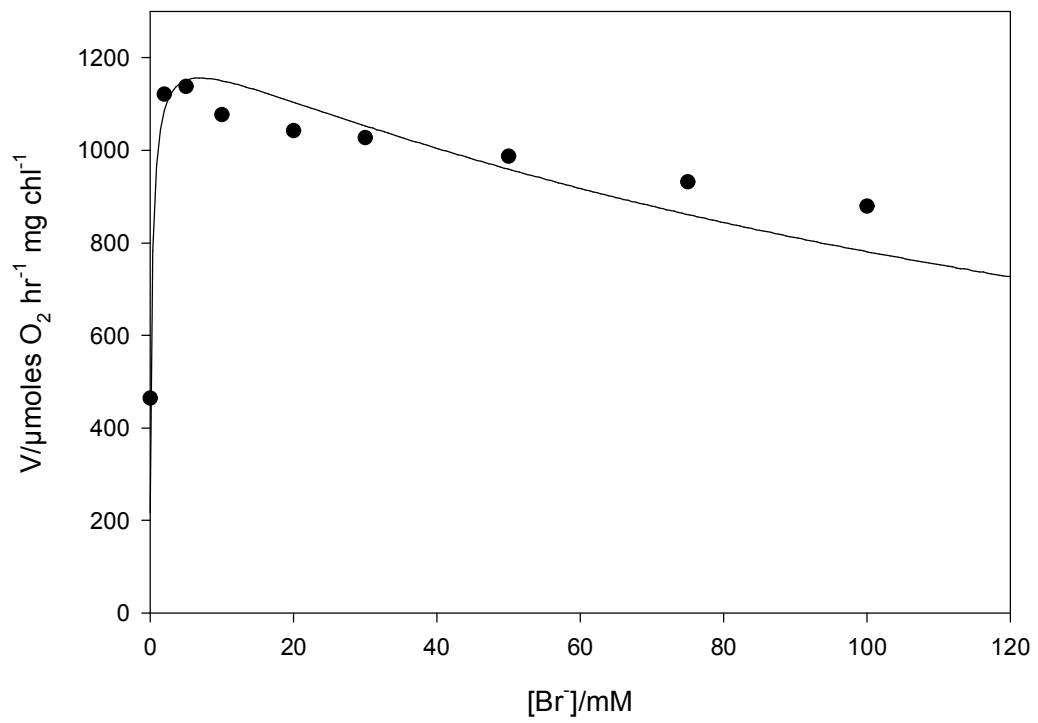


Figure 11B: Br⁻ activation of PS II that was Cl⁻ depleted by dialysis after Br⁻ treatment

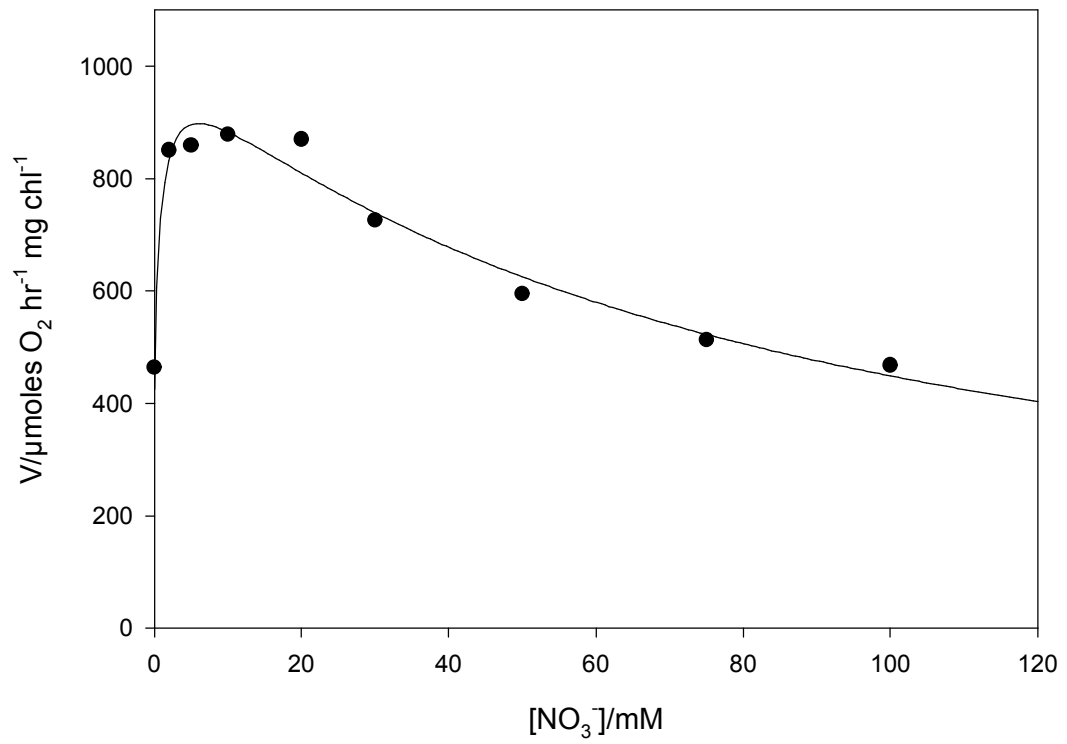


Figure 11C: NO₃⁻ activation of PS II that was Cl⁻ depleted by dialysis after Br⁻ treatment

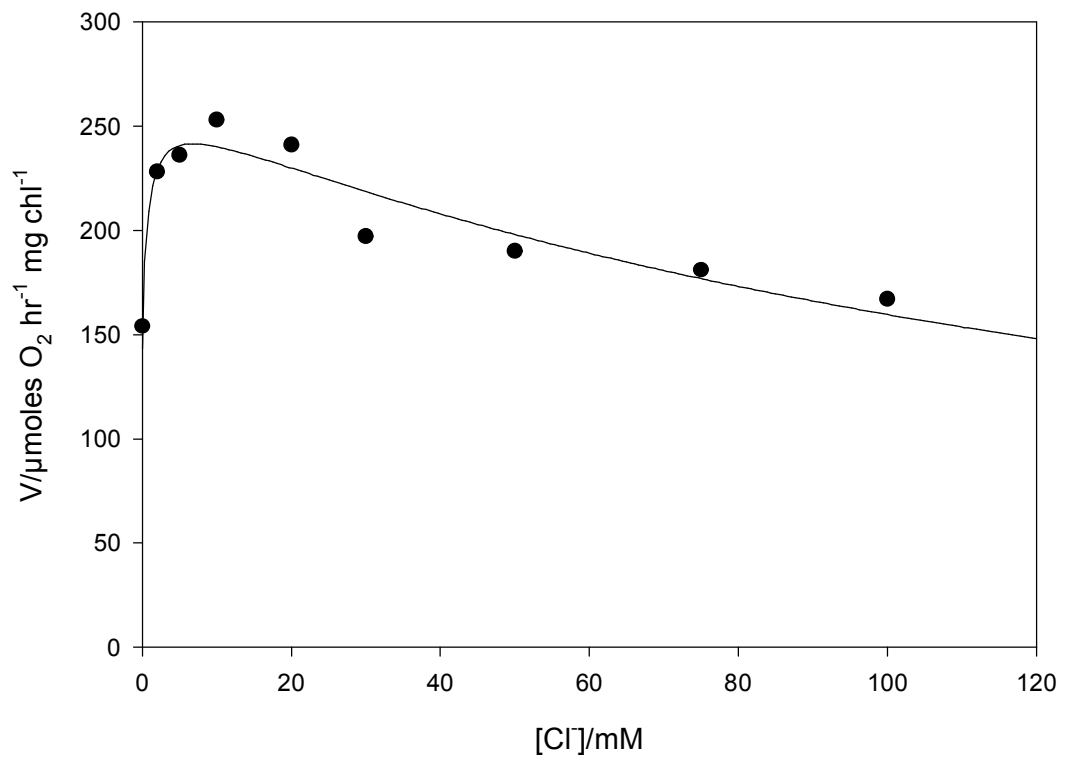


Figure 12A: Cl⁻ activation of PS II that was Cl⁻ depleted by dialysis (no pretreatment)

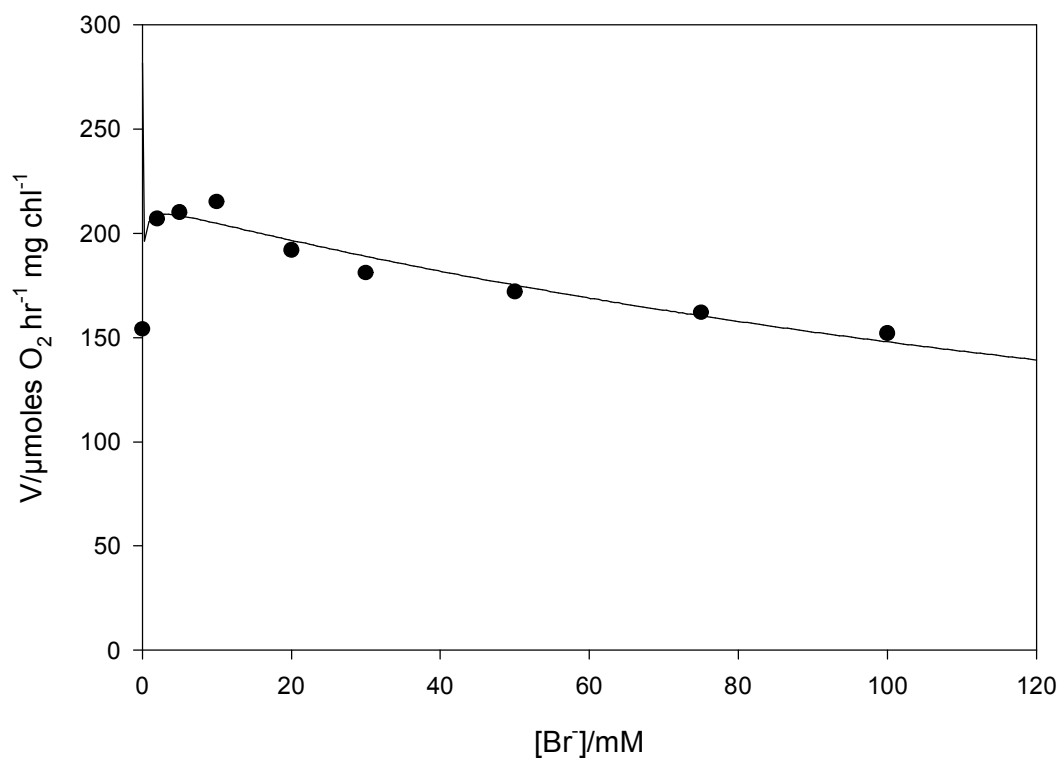


Figure 12B: Br^- activation of PS II that was Cl^- depleted by dialysis (no pretreatment)

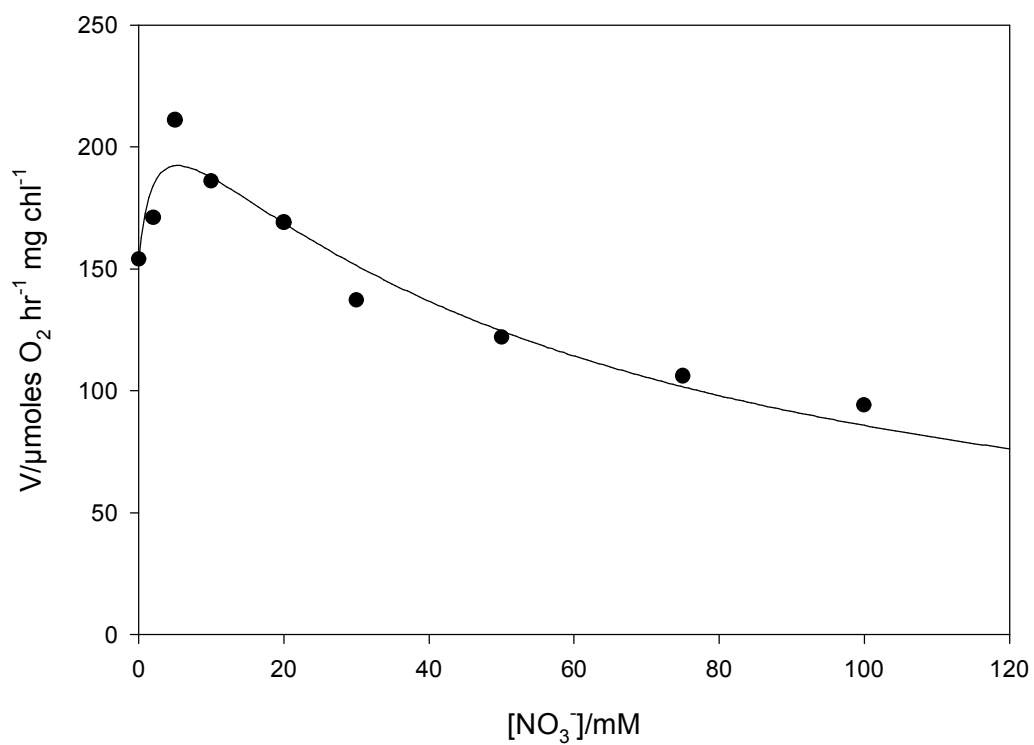


Figure 12C: NO₃⁻ activation of PS II that was Cl⁻ depleted by dialysis (no pretreatment)

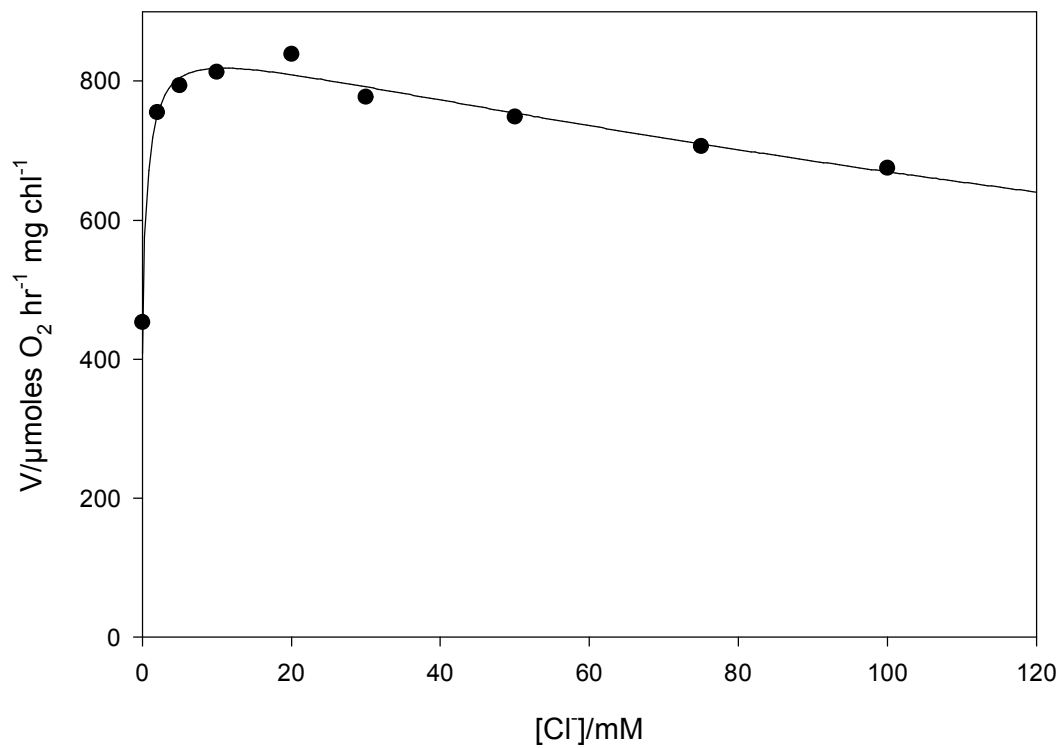


Figure 13A: Cl⁻ activation of PS II after 6 washes in Cl⁻ free buffer

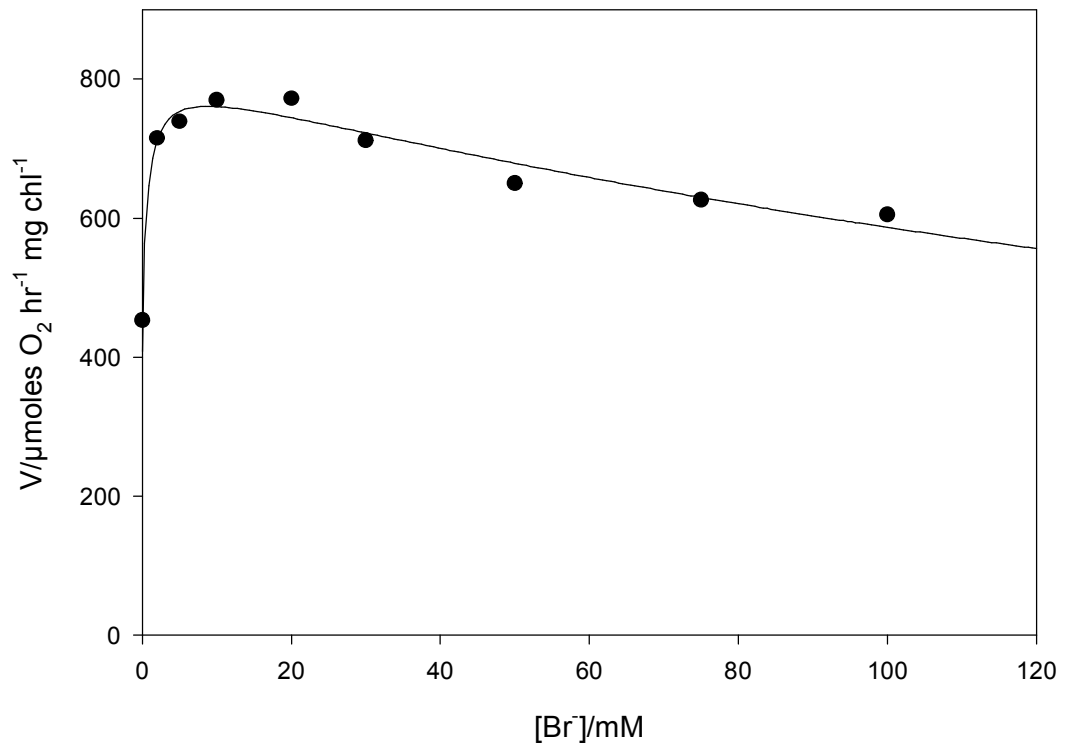


Figure 13B: Br⁻ activation of PS II after 6 washes in Cl⁻ free buffer

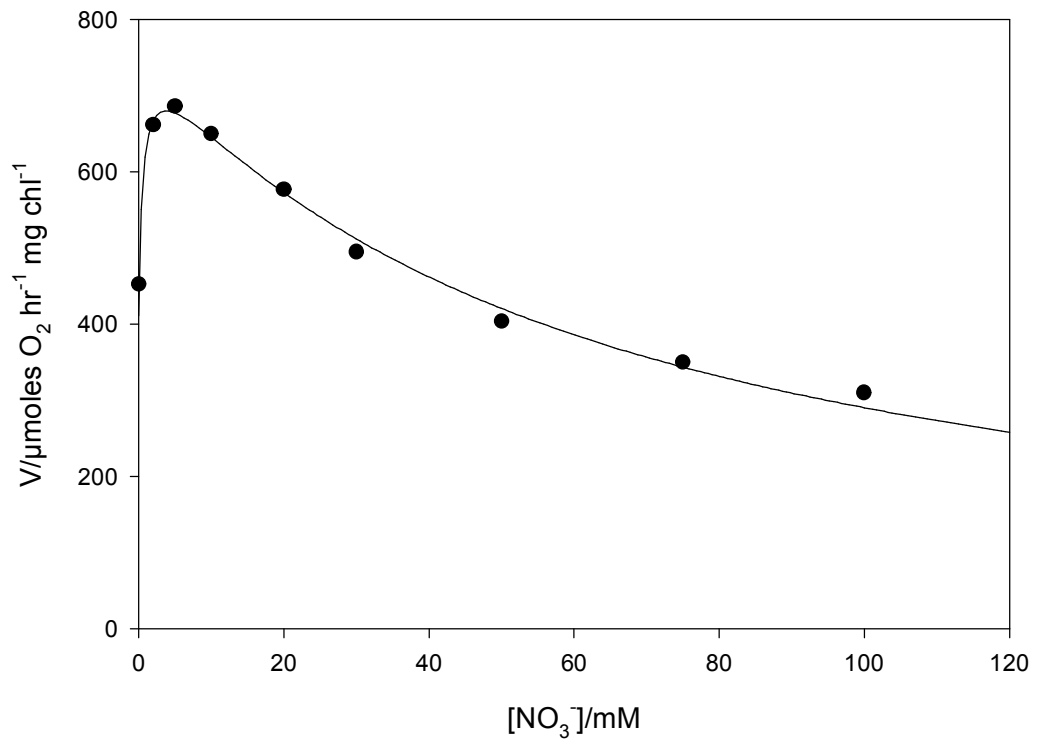


Figure 13C: NO₃⁻ activation of PS II after 6 washes in Cl⁻ free buffer

SDS-PAGE analysis of PS II after dialysis

To confirm that PS II remained intact, with the 17 and 23 kDa subunits bound, after dialysis to remove Cl^- , SDS-polyacrylamide gel electrophoresis was carried out. The preparation chosen for this analysis was the one that had been pretreated with NO_3^- , since this showed the greatest effect on the kinetics of activation. We were particularly concerned with confirming the presence of the 17 and 23 kDa subunits, since these are associated with the retention of Cl^- at the OEC and they are the easiest subunits to remove. In addition, the presence of the 17 and 23 kDa subunits in Cl^- depleted PS II could help explain why there was still some activity after dialysis, since their presence may block removal of Cl^- from PS II.

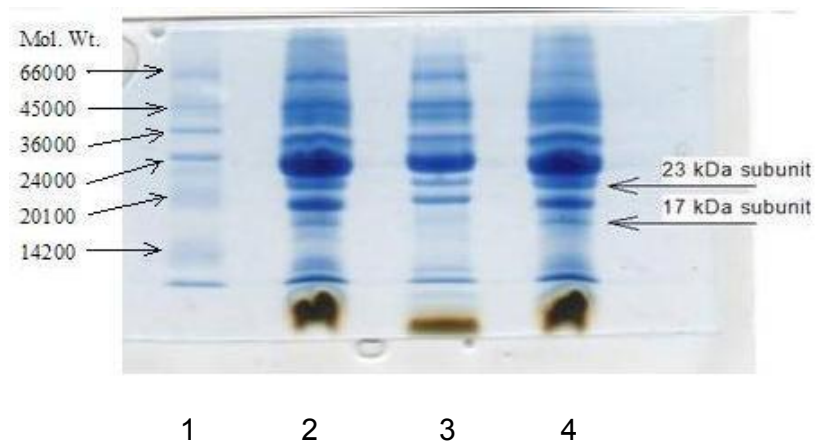


Figure 14: SDS-PAGE of PS II after different treatments

**1. Molecular weight standard 2. Intact PS II 3. NaCl-washed PS II 4. Cl^- depleted PS II
using NO_3^- pretreatment**

PS II depleted of Cl^- by dialysis after NO_3^- pretreatment was analyzed by SDS-PAGE as described in Materials and Methods (Figure 14). It was compared with a molecular weight standard (lane 1) and two PS II samples that served as positive and negative controls for comparison. One was intact PS II (lane 2) and the other was NaCl-washed PS II (lane 3), from which the 17 and 23 kDa subunits had been removed completely (A band at 24 kDa corresponds to an intrinsic membrane subunit). As can be seen in lane 4 the 17 and 23 kDa subunits remained bound to the PS II that had been Cl^- depleted after NO_3^- pretreatment.

Study of the S_2 state EPR signals in PS II depleted of Cl^- after NO_3^- treatment

To better understand the effect of anion activators in Cl^- depleted PS II, the S_2 state EPR signals were examined in the presence of Cl^- , Br^- and NO_3^- . In general, the multiline EPR signal is correlated with activation by Cl^- or other anion, while the $g=4.1$ signal is observed in both the presence or absence of activating anion.

For EPR experiments, we chose the PS II that had been Cl^- depleted after NO_3^- treatment for these experiments, because of its unusual activation behavior. Samples of this preparation were prepared for EPR spectroscopy by adding 25 mM NaCl, NaBr, NaNO_3 or no anions as described in Materials and Methods. The oxygen evolution activity was tested and compared with the

kinetic analyses of the previous section.

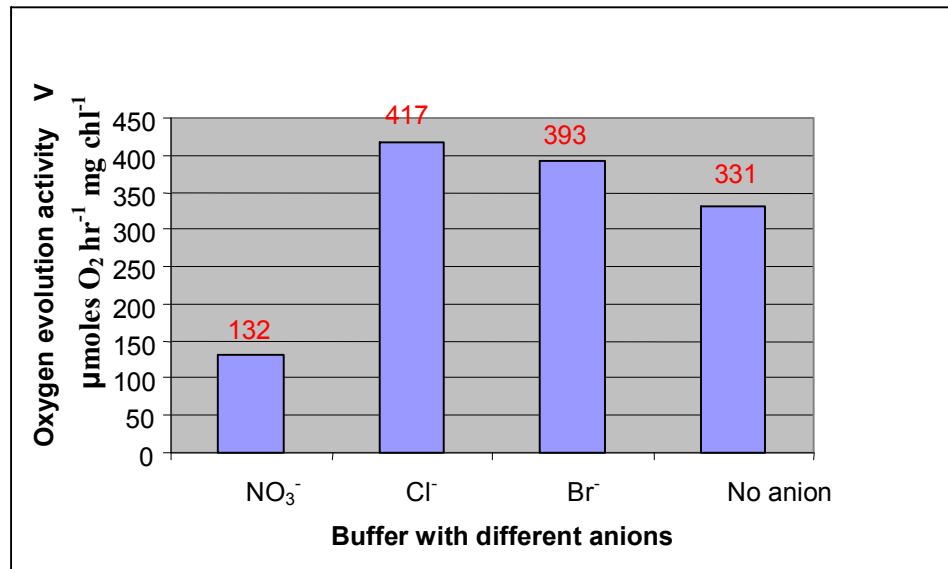


Figure 15: Oxygen evolution activity of PS II that was Cl⁻ depleted by dialysis after NO₃⁻ treatment after readdition of 25 mM anion.

Normally, the oxygen evolution activity of the sample with buffer containing NO₃⁻ is expected to be greater than that of the sample with no anion, but here we obtained the reversed result. This experiment was repeated with the same result. The order of activation of the four samples was Cl⁻>Br⁻>no anion>NO₃⁻. The low activity in the presence of NO₃⁻ is explained by the almost complete lack of activation by NO₃⁻ for this preparation, with inhibition dominating, as seen in Figure 10C. After the addition of 25 mM NO₃⁻ the activity of the preparation was more inhibited than in the absence of added anion.

The S_2 state EPR signals were examined, for the same samples using difference spectroscopy of the illuminated sample minus the dark adapted sample (Figure 16). The multiline signal is present in all spectra except for that of the NO_3^- containing sample and it has the highest intensity in the Cl^- containing sample. The signal at $g=4.1$ is observed in all four samples, although it has the lowest intensity in the Br^- containing sample. Signal heights were measured for both signals and compared using the percentage with respect to the Cl^- containing sample as 100%. Since the various samples had different chlorophyll concentrations the heights were corrected for concentration, normalizing to the height of the Cl^- containing sample (Table 4).

In Table 5, the normalized signal heights are compared with the oxygen evolution activity. The height of the multiline signal was found to follow the same trend as the oxygen evolution with $\text{Cl}^- > \text{Br}^- > \text{no anion} > \text{NO}_3^-$.

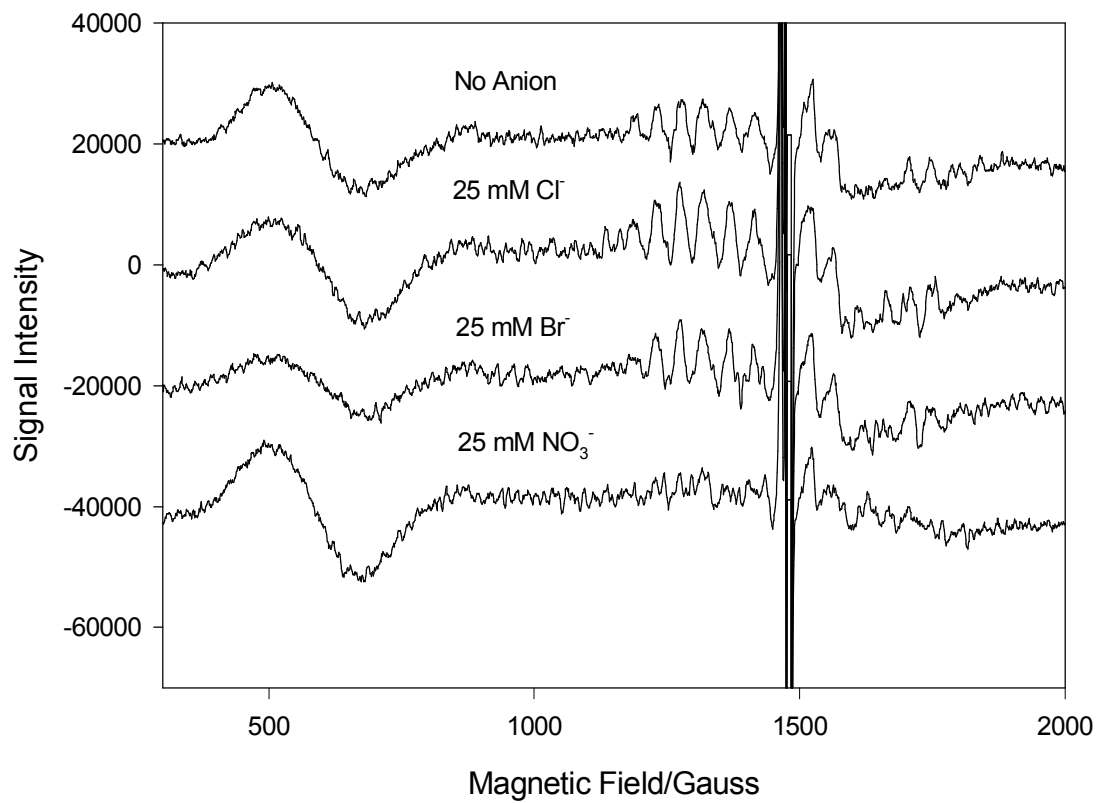


Figure 16: S₂ state EPR signals for Cl⁻ depleted PS II with NO₃⁻ pretreatment. The spectra shown were obtained by taking the difference between the spectrum of the illuminated sample minus that of the dark-adapted sample.

Table 4: Measurement of the S₂ state EPR signals in PS II after Cl⁻ depletion using NO₃⁻ pretreatment in the presence of 25 mM anion from Figure 16

anion		none	Cl ⁻	Br ⁻	NO ₃ ⁻
concentration (mgChl/ml)		1.12	0.995	1.26	1.28
multiline signal	height	7980	12628	11438	~0
	normalized height*	7083	12628	9068	~0
	% normalized height	56.1%	100%	71.8%	~0
g=4.1 signal	height	18852	17891	10821	22585
	normalized height*	16733	17891	8579	17556
	% normalized height	93.5%	100%	47.9%	98.1%

* corrected for difference in chlorophyll concentration

Table 5: Comparison of the S₂ state EPR signals and oxygen evolution activity for the samples shown in Figure 16 and Table 4

anion	Multiline normalized heights (%)	g=4.1 normalized heights (%)	O ₂ evolution activity (%)
None	56.1%	93.5%	79.4%
Cl ⁻	100%	100%	100%
Br ⁻	71.8%	47.9%	94.2%
NO ₃ ⁻	~0	98.1%	31.7%

CHAPTER V

DISCUSSION

My research goal was to investigate methods for removing Cl^- completely from PS II and to characterize the effects of the treatments for Cl^- removal.

The dialysis method did not successfully remove the Cl^- completely from PS II in any case, thus it was not completely effective. The best result was found for PS II that had been dialyzed after Br^- pretreatment, which had about 40% residual activity. Table 2, $V_0/(V_0+V_{\text{max}})$ represents the residual activity. It can be seen that Cl^- depletion after Br^- pretreatment resulted in the lowest residual activity, which Cl^- depletion after NO_3^- pretreatment resulted in the largest value, even bigger than the treatment by no added anion. This means that Cl^- depletion after Br^- pretreatment was the most successful method to remove Cl^- from PS II and Cl^- depletion after NO_3^- pretreatment was the least effective method.

However methods used by researchers in other labs have also not been successful in depleting PS II of Cl^- completely. Lindberg and Andreasson carried out first experiments for Cl^- depletion of PS II by dialysis in the absence of anion pretreatment.⁽²⁰⁾ They measured the oxygen evolution activity of the

dialyzed PS II samples with the addition of Cl^- in the concentration range from 0 to 25 mM. Their results for Cl^- activation were similar to ours for Cl^- concentrations below 25 mM, which was the highest concentration they tested.

Inhibition of PS II due to a high concentration of anion activator has been observed in previous studies. In a study of the dependence of oxygen evolution activity on Cl^- concentration in untreated, NaCl-treated and (urea + NaCl)-treated PS II samples, Miyao and Murata found that the oxygen evolution activity dropped with increasing with Cl^- concentrations over 10 mM. ⁽¹⁶⁾ Similar results were found in a second study by Miyao and Murata, using NaCl-treated PS II samples in the presence of 1.0 mM Ca^{2+} . ⁽¹¹⁾ In this case, the oxygen evolution activity increased with the addition of Cl^- , up to about 30 mM Cl^- concentration, then decreased with higher concentrations.

Iodide is another anion that can activate PS II in place of Cl^- , but with inhibitory effects at lower concentrations than Cl^- . Ikeuchi and coworkers measured the oxygen evolution activity with the addition of I^- to the NaCl-treated PS II samples, observing inhibitory effects. The oxygen evolution activity dropped to a level that was lower than the initial activity V_0 at about 25 mM I^- concentration. ⁽³³⁾ Bryson et al described the inhibitory effects of iodide from a second anion site in a study of oxygen evolution in Cl^- -depleted intact PS II. Using a substrate inhibition model, they found kinetic parameters: $K_M =$

1.5 mM, $K_I = 8.8$ mM. They found that I^- could work as an activator at low concentrations and also as an inhibitor at high concentrations.⁽³⁴⁾

In addition to the least effective method to remove Cl^- from PS II, (with the highest value of $V_0/(V_0+V_{max})$), PS II that was Cl^- depleted after NO_3^- pretreatment showed the greatest change in kinetic parameters. In particular, activation of this preparation by NO_3^- was especially poor due to a very high K_M value (8.4 mM). This might be explained by the binding of NO_3^- in place of Cl^- as a result of the pretreatment. Also in all three experiments, the additions of NO_3^- have the biggest K_M value and the lowest K_I value, such that all residual activity V_0 was promoted by NO_3^- that was already bound. Then the further addition of NO_3^- did not activate further, but only inhibited.

In addition to being the most effective method to remove Cl^- from PS II, (with the lowest $V_0/(V_0+V_{max})$ value), PS II that was Cl^- depleted after Br^- pretreatment was the most active preparation. It showed the largest V_{max} value (even given possible systematic error) for all activating anions and the highest overall oxygen evolution activity, which indicates that it was the healthiest preparation. This suggests that Br^- facilitated Cl^- removal as we hoped to achieve, although perhaps not completely or with replacement of Cl^- with Br^- . The result also suggests that Br^- protected against loss of activity during the treatment.

Using PS II that was Cl^- depleted after NO_3^- pretreatment, we found that

the S_2 state multiline EPR signal corresponded to the measurement of the oxygen evolution activity whereas the $g=4.1$ signal did not. The order of multiline signal heights matched the order of activity in the presence of 25 mM anion added: $Cl^- > Br^- > \text{no anion} > NO_3^-$. Both the O_2 evolution activity and EPR multiline signal intensity in the presence of 25 mM NO_3^- were lower than in the absence of added anion. This observation is consistent with the suggestion given above that NO_3^- displaced tightly bound Cl^- during dialysis. As with O_2 evolution activity, the NO_3^- that displace Cl^- during the Cl^- promoted formation of the multiline signal in the absence of added anion, while further NO_3^- only suppressed the signal formation.

Lindberg and Andreasson also studied the effects on the S_2 state EPR signals in PS II that was Cl^- depleted by dialysis. In addition to loss about 65% activity⁽³⁰⁾, the depletion Cl^- resulted in a shift in signal intensity toward the $g=4.1$ signal at the expense of the multiline signal. The original distribution of the EPR signals was immediately restored after the addition of Cl^- or Br^- to the depleted PS II samples. This result is similar to ours, although we did not observe an increase in the $g=4.1$ signal.

Ono and coworkers also carried out an EPR study of PS II membranes in which Cl^- had been replaced by other anions.⁽³⁵⁾ They found that the S_2 state multiline signal was induced in Cl^- containing membranes and Br^- -substituted membranes, but its amplitude was decreased to less than 10%

in NO_3^- -substituted membranes. The $g=4.1$ signal, in NO_3^- -substituted membranes was markedly enhanced, but its amplitude was decreased to less than 70% in Br^- -substitute membranes. These results are similar to our results, although again we did not observe an increase in the $g=4.1$ signal.

REFERENCES

1. R. E. Blankenship. (2002) *Molecular Mechanisms of Photosynthesis*. Blackwell Science, Oxford.
2. W. Hillier and G. T. Babcock. (2001) "Photolytic Reaction Centers". *Plant Physiology* 125, 33-37.
3. P. Jordan, P. Fromme, H. T. Witt, O. Klukas and W. Saenger. (2001) "Three-dimensional Structure of Cyanobacterial Photosystem I at 2.5 Å resolution". *Nature* 411, 909-917.
4. R. D. Britt. "Oxygen Evolution". (1996) *Oxygenic photosynthesis: The light reactions*, Kluwer Academic Publishers, Netherlands, 137-164.
5. <http://www.bio.ic.ac.uk/research/barber/psIIimages/PSII.html>
6. B. Kok, B. Forbush and M. McGloin. (1970) "Cooperation of charges in photosynthetic O₂ evolution – I. A linear four step mechanism". *Photochemistry Photobiology* 11, 457-475.
7. K. N. Ferreira, T. M. Iverson, K. Maghlaoui, J. Barber, S. Iwata. (2004) "Architecture of the Photosynthetic Oxygen-Evolving Center". *Science*, 303, 1831-1838.
8. A. Zouni, H. T. Witt, J. Kern, P. Fromme, N. Krauss, W. Saenger, P. Orth. (2001) "Crystal structure of photosystem II from *Synechococcus elongatus* at 3.8 Å resolution". *Nature* 409, 739-743.

9. T. M. Bricker and D. F. Ghanotakis. (1996) "Introduction to Oxygen Evolution and the Oxygen-Evolving complex". *Oxygenic Photosynthesis: The Light Reactions*, Kluwer Academic Publishers, Netherlands, 113-136.
10. N. Mizusawaa, T. Yamashitab and M. Miyao. (1999) "Restoration of the high-potential form of cytochrome b559 of photosystem II occurs via a two-step mechanism under illumination in the presence of manganese ions". *Biochimica et Biophysica Acta* 1410, 273-286.
11. M. Miyao and N. Murata. (1989) "The mode of binding of three extrinsic proteins of 33 kDa, 24 kDa and 18 kDa in the Photosystem II complex of spinach". *Biochimica et Biophysica Acta*, 977, 315-321.
12. K. Kavelaki and D. F. Ghanotakis. (1991) "Effect of the manganese complex on the binding of the extrinsic proteins (17, 23 and 33 kDa) of Photosystem II". *Photosynthesis Research* 29, 149-155.
13. M. Miyao and Y. Inoue. (1983) "Partial disintegration and reconstitution of the photosynthetic oxygen evolution: Effect of artificial electron acceptors on the photoactivation yield of NH₂OH-treated wheat Photosystem II membranes". *Biochimica et Biophysica Acta*, 1056, 47-56.
14. M. Miyao and N. Murata. (1984) "Calcium ions can be substituted for the 24-kDa polypeptide in photosynthetic oxygen evolution". *Biochimica et Biophysica Acta*, 168, 118-120.
15. C. M. Waggoner and C. F. Yocum. (1987) "Selective depletion of

- water-soluble polypeptides associated with Photosystem II". *Progress in Photosynthesis Research*, Vol I, 685-688.
- 16.M. Miyao and N. Murata. (1985) "The Cl⁻ effect on photosynthetic oxygen evolution: interaction of Cl⁻ with 18-kDa, 24-kDa and 33-kDa proteins". *Biochimica et Biophysica Acta* 180, 303-308.
- 17.P. E. Siegbahn, R. H. Crabtree. (1999) "Manganese Oxyl Radical Intermediates and O-O Bond Formation in Photosynthetic Oxygen Evolution and a Proposed Role for the Calcium Cofactor in Photosystem II". *Journal of the American Chemical Society*, 121, 117.
- 18.P. E. Siegbahn. (2002) "Quantum chemical studies of manganese centers in biology". *Current Opinion in Chemical Biology*, 6, 227.
- 19.J. H. Robbleee, R. M. Cince, V. K. Yachandra. (2001) *Biochimica et Biophysica Acta*, 1503, 7.
- 20.K. Lindberg, T. Vanngard and L. E. Andreasson. (1993) "Studies of the slowly exchanging chloride in Photosystem II of higher plants". *Photosynthesis Research* 38: 401-408.
- 21.C. Critchley. (1985) 'The role of chloride in photosystem II". *Biochimica et Biophysica Acta* 811, 33-46
- 22.K. Kawamoto, J. Mano and K. Asada. (1995) "Photoproduction of the azidyl radical from the azide anion on the oxidizing side of Photosystem II and suppression of photooxidation Tyrosine-Z by the azidyl radical". *Plant and Cell*

Physiology 36 1121 - 1129.

23. N. J. Bunce. (1987) "Introduction to the interpretation of electron spin resonance spectra of organic radicals". *Journal of chemical education*, 64, 907-914.
24. G. C. Dismukes and Y. Siderer. (1981) "Intermediates of a polynuclear manganese center involved in photosynthetic oxidation of water". *Proceedings of the National Academy of Sciences of the United States of America*, 78(1): 274-278.
25. J. L. Casey and intermediate in photosynthetic oxygen evolution". *Biochimica et Biophysica Acta*, K. Sauer. (1984) "EPR detection of a cryogenically photogenerated 767, 21-28.
26. D. H. Kim, R. D. Britt, M. P. Klein and K. Sauer. (1990) "The $g=4.1$ EPR signal of the S_2 state of the photosynthetic oxygen evolving transport and on hydroxylamine inhibition". *Biochimica et Biophysica Acta*, 502, 198-210.
27. D. H. Kim, R. D. Britt, M. P. Klein and K. Sauer. (1992) "The manganese site of the photosynthetic oxygen-evolving complex probed by EPR spectroscopy of oriented Photosystem II membranes: The $g=4$ and $g=2$ multiline signals". *Biochemistry* 31, 541-547.
28. J. L. Zimmermann and A.W. Rutherford. (1984) "EPR Studies of the Oxygen-Evolving Enzyme of Photosystem II". *Biochimica et Biophysica Acta*, 767, 160-167.

29. A. Haddy, R. A. Kimel and R. Thomas. (2000) "Effects of Azide on the S₂ State EPR Signals from Photosystem II". *Photosynthesis Research*, 63: 35-45.
30. K. Lindberg and L. E. Andreasson. (1996) "A One-Site, Two-State Model for the Binding of Anions in Photosystem II". *Biochemistry*, 199, 35, 14295-14267.
31. Berthold, Babcock and Yocum. (1981) "A highly resolved, oxygen-evolving Photosystem II preparation from spinach thylakoid membranes". *FEBS Letter*, 134, 231-234.
32. Kashino, Koike and Satoh. (2001) "An improved sodium dodecyl sulfate polyacrylamide gel electrophoresis system for the analysis of membrane protein complexes". *Electrophoresis* 22, 1004-1007.
33. M. Ikeuchi, H. Koike and Y. Inoue. (1988) "Iodination of D1 (herbicide-binding protein) is coupled with photooxidation of ¹²⁵I⁻ associated with Cl⁻-binding site in Photosystem-II water-oxidation system". *Biochimica et Biophysica Acta*, 932, 160-169.
34. D. I. Bryson, N. Doctor, R. Johnson, S. Baranov and A. Haddy. (2005) "Characteristics of iodide activation and inhibition of oxygen evolution by Photosystem II". *Biochemistry*, 44, 7354-7360.
35. T. Ono, H. Nakayama, H. Gleiter, Y. Inoue and A. Kawamori. (1987) "Modification of the properties of S₂ state in Photosynthetic O₂-evolving center by replacement of chloride with other anions". *Biochemistry and Biophysics*, 256, 618-624.